AN ALGORITHM FOR THE SELECTION OF MULTIPHASE STEEL PARAMETERS

AN AI-BASED OPTIMIZATION FRAMEWORK FOR OPTIMAL COMPOSITION AND THERMOMECHANICAL PROCESSING SCHEDULE FOR SPECIALIZED MICRO-ALLOYED MULTIPHASE STEELS

By MARTHA KAFUKO, B.Eng.

A Thesis Submitted to the Department of Mechanical Engineering and the School of Graduate Studies of McMaster University in Partial Fulfilment of the Requirements for the Degree of Master of Applied Science

McMaster University MASTER OF APPLIED SCIENCE (2023), Hamilton, Ontario

TITLE:	An AI-Based Optimization Framework for Optimal Composition and Thermomechanical Processing Schedule for Specialized Micro-Alloyed Multiphase Steels
AUTHOR:	Martha Kafuko, B.Eng. (McMaster University)
SUPERVISOR:	Dr. Seshasai Srinivasan
NUMBER OF PAGES:	xx, 98

Lay Abstract

This research aims to develop an AI-based functional integrated with a heuristic algorithm that optimizes parameters to meet desired mechanical properties and cost for steels. The developed algorithm generates new alloys which meet desired mechanical property targets by considering alloy composition and heat treatment condition inputs. Used in combination with machine learning models for the mechanical property and microstructure prediction of new alloys, the algorithm successfully demonstrates its ability to meet specified targets while achieving cost savings. The approach presented has significant implications for the steel industry as it offers a quick method of optimizing steel production, which can reduce overall costs and improve efficiency. The integration of machine learning within the algorithm offers a different way of designing new steel alloys which has the potential to improve manufactured products by ultimately improving their performance and quality.

Abstract

Steel is an important engineering material used in a variety of applications due to its mechanical properties and durability. With increasing demand for higher performance, complex structures, and the need for cost reduction within manufacturing processes, there are numerous challenges with traditional steel design options and production methods with manufacturing cost being the most significant. In this research, this challenge is addressed by developing a micro-genetic algorithm to minimize the manufacturing cost while designing steel with the desired mechanical properties. The algorithm was integrated with machine learning models to predict the mechanical properties and microstructure for the generated alloys based on their chemical compositions and heat treatment conditions. Through this, it was demonstrated that new steel alloys with specific mechanical property targets could be generated at an optimal cost.

The research's contribution lies in the development of a different approach to optimize steel production that combines the advantages of machine learning and evolutionary algorithms while increasing the number of input parameters. Additionally, it uses a small dataset illustrating that it can be used in applications where data is lacking. This approach has significant implications for the steel industry as it provides a more efficient way to design and produce new steel alloys. It also contributes to the overall material science field by demonstrating its ability in a material's design and optimization. Overall, the proposed framework highlights the potential of utilizing machine learning and evolutionary algorithms in material design and optimization.

Dedicated to my support system for their unwavering love and encouragement.

Acknowledgments

I would like to thank my supervisor, Dr Seshasai Srinivasan, for his support, guidance, and expertise that have been a driving force behind the success of this research. His mentorship and willingness to take me on as a student have been instrumental in bringing my thesis to where it stands today. I would also like to extend my thanks to Dr. Mohamed Elbestawi for his input and suggestions which have helped shape and strengthen this research.

My deepest appreciation goes to my family: my loving parents Tom and Grace Wanyama, whose unwavering love, support, and encouragement have been instrumental throughout my academic journey. I am also grateful to my siblings Tom M. Wanyama, Paul Barasa, and Elizabeth Anyango for their constant motivation and belief in my abilities. Special thanks go to my best friend and partner, Alexandru Barsan, who has been a constant source of strength and inspiration on this adventure. Without this support system, this achievement would not have been possible.

Table of Contents

List of Figures

List of Tables

Abbreviations and Symbols

Below is a list of all the abbreviations and symbols used within.

List of Abbreviations

ANN	Artificial Neural Network
C	Celsius
CR	Cooling Rate
GA	Genetic Algorithm
HSLA	High Strength Low Alloy
HV	Vicker's Hardness
IOSO	Indirect Optimization Self-Organization
K	Kelvin
MC	Manufacturing Cost
MLP	Multi-layer Perceptron
MSE	Mean Squared Error
OEB	Ontario Energy Board
ROH	Reduce Order Hardness
ROM	Reduced Order Model
s	Seconds
SA	Simulated Annealing
STD	Standard Deviation
TE	Tensile Elongation

TMCP	Thermomechanical Controlled Processing
TMP	Thermomechanical Processing
TS	Tensile Strength
TTT	Time-Temperature-Transformation
UTS	Ultimate Tensile Strength
YS	Yield Strength

List of Symbols

co	Cost Exponent
f	Cost Function
Co	Cost Weight
e	Elongation Exponent
E	Elongation Weight
h	Hardness Exponent
H	Hardness Weight
x	Input Parameters
μ	Micro
ς	Penalty Parameters
0	Target Values

s	Tensile Strength Exponent
S	Tensile Strength Weight

Declaration of Academic Achievement

I, Martha Kafuko, declare that the contents written herein, submitted in partial fulfillment of the requirements for the degree of Master of Applied Science, at McMaster University, are a record of my original work performed solely by me with the guidance of my supervisor Dr. Seshasai Srinivasan. This is the true copy of the thesis which includes final revisions, as accepted by the reviewers. Further, I understand that this thesis shall be made available to the public via MacSphere.

Chapter 1 Introduction

1.1 Background Overview

Used in a variety of industries, steel is a crucial material due to its combination of strength, toughness, and durability. In fact, due to its malleability, it is typically used in most construction and automotive projects with roughly 55% of the weight of passenger cars being made of it. Further, it is used in the creation of shipping containers, various appliances, and machinery [1]. Therefore, it is important that the design of steel achieves the desired mechanical properties, based on its application, at a reasonable cost. To ensure this, the production process must be optimized. As such, in recent years, there has been an increased focus on using various computational methods to optimize this process, resulting in more efficient, and importantly cost-effective, steel production.

Since traditional optimization techniques are usually computationally expensive and require extensive experimentation, the development of optimization techniques such as genetic algorithms (GAs), have become an efficient way to find optimal solutions to steel optimization problems by designing new alloys with desired properties. To accomplish this, GAs take on a natural selection and genetic inspired approach to search for optimal combinations. In the case of this research, these combinations are of alloying elements and heat treatment conditions. To improve the algorithms performance, the use of machine learning models was also applied. These models were used for the prediction of the mechanical properties and microstructure of the new alloys. With this, GAs

demonstrated their ability to design new materials that meet specified targets with cost savings.

While GAs have shown to be promising in the optimization of steel, they typically also require many evaluations, which is time consuming and ultimately computationally expensive. To address this, micro-genetic algorithms (μGA) have been proposed as a more efficient technique. As a subset of GAs, these algorithms use smaller populations and fewer iterations applied to a local search procedure resulting in faster convergence towards an optimal solution. As such, they are effective for use in the steel optimization problem.

1.2 Research Motivation and Objective

An increased demand for cost effective steels that meet desired mechanical properties has driven the need for the optimization of steel production. Since traditional experimental methods – trial and error – are both time consuming and require a significant number of resources, new methods that are more practical in the current market are being researched. Therefore, the development of new techniques that are efficient and effective are necessary to meet current demand. Techniques utilizing machine learning such as Neural Networks (NNs), support vector machines etc. have been used to predict the mechanical properties of steel. However, such techniques do not consider or provide cost optimization capabilities. On the other hand, although the use of GAs has proved to be beneficial in the cost optimization of steel alloys, they are computationally resource intensive.

Therefore, the objective of this research is to develop a μGA that can overcome the limitations of traditional GAs. It combines the advantages of utilizing machine learning

techniques for prediction and optimization techniques for generation. The μGA shall be used to optimize parameters for mechanical properties. Further, it shall also be used to optimize for the cost of steel production while ensuring that desired mechanical property targets are still met. As such, its success will provide a means for the industry to optimize for steel products more efficiently and at a reduced cost.

1.3 Research Contributions and Novelty

The main contributions of this research are summarized as follows:

1. The development of a μGA for steel optimization: This research develops a μGA for the optimization of steel mechanical properties and cost by considering the chemical composition (alloying elements) and heat treatment conditions. It increases the number of inputs parameters by including more alloying elements and utilizes continuous cooling profiles rather than isothermal condition to get the optimal cost.
2. The development of Reduced Order Models (ROMs) for mechanical property prediction: ROMs for the prediction of three mechanical properties namely, hardness, tensile strength, and elongation were developed using machine learning and existing correlation equations. This research expands on existing work that usually focuses on one or two properties and incorporates machine learning for more accurate results.
3. The use of Artificial Neural Networks (ANNs) to obtain the mechanical properties and microstructure phase fractions: ANNs are used to predict the mechanical properties and microstructures of the new alloys. This is

accurately achieved with a relatively small training dataset. As such these models enable the optimization algorithm to predict properties of new alloys without the need of experimental tests which could be costly.

4. The optimization of steel for mechanical properties and cost: The developed algorithms and machine learning models provide an alternative to costly experimental testing that would be required to determine suitable parameters to obtain steels with desired mechanical properties. As such they improve efficiency while reducing cost that is needed in the steel industry.

Overall, the novelty of this research is through the development of a μGA that incorporates machine learning techniques to design steels with desired mechanical property at the least manufacturing cost. The approach presented in this thesis offers a different and effective way to optimize for steel that can potentially reduce the cost of its production and provide efficiencies.

1.4 Thesis Structure

The thesis is organized as follows: Chapter 1 provides an overview of the research topic, its motivation and objectives, and contributions. Chapter 2 provides an in-depth review of the relevant literature on steel optimization. This includes the effects of chemical compositions and microstructure on mechanical properties, how machine learning is used for mechanical property predictions, as well as an overview on the use of GAs in steel optimization. Chapter 3 outlines the methodology used for creating the algorithm and its analysis. The algorithm's validation, and results and discussion are presented in Chapter 4. This chapter also focuses on the method's limitations and proposed future work. Lastly,

Chapter 5 summarizes the overall findings, outlines the implication for practical applications, and provides recommendations for future research. The appendices provide an outline of the hardness and microstructure NN model design, any relevant pseudo code, and general information required in the optimization analysis such as cost, and software used.

Chapter 2 Literature Review

2.1 Steel Optimization Overview

Optimizing the properties of steel is an essential task that aims to improve its mechanical and physical properties. This is often accomplished by manipulating its chemical composition, microstructure, and/or Thermomechanical Processing (TMP) conditions – also known as heat treatment conditions –, utilizing a combination of experimental and computational techniques with a goal of creating new materials that exhibit desired mechanical properties. As such, there has been a growing body of research specifically dedicated to studying the optimization of steel through the modification of its chemical composition and heat treatment conditions, with the goal of enhancing its performance in various industrial applications.

Numerous approaches, including empirical and mathematical modelling methods, have been taken to optimize a steel's properties. Empirical methods use trial-and-error experiments to determine properties that produce optimal solutions whereas mathematical modelling approaches are employed to predict these same properties. Recently however, new studies have explored the use of complex computational algorithms and machine learning to target these problems with genetic algorithms gaining popularity due to their ability to quickly find optimal solutions [2]. According to Adeli et al. [3], there are three major strategies that can be used for the cost optimization of steel structures namely, fuzzy logic, genetic algorithms, and parallel computing. Fuzzy logic and genetic algorithms can be used to optimize cost and other target parameters, while parallel computing is used to

accelerate the optimization process. The selection of the method typically depends on the application. For example, fuzzy logic was shown to be more advantageous in applications such as the optimization of steel in seismic design applications and in the optimization of composite floors among others. On the other hand, GAs have shown to be successful in the design of steel not only for seismic design applications and other structures but for the design of bolts and plates.

Overall, there are several methods that can be used for steel optimization – each with its own advantages, disadvantages, and limitations. Ultimately, the approach used depends on the specific goals that need to be met taking into consideration the constraints of the optimization problem. In this research, the approach taken focuses on achieving target properties while minimizing cost using a genetic algorithm. Therefore, the rest of the sections will focus on steel optimization using this optimization strategy.

2.2 Steel Composition and Microstructure Effects on Mechanical Properties

Steel composition and microstructure play an important role in determining its mechanical properties. Since, properties such as strength, toughness, ductility, elongation etc., are all crucial in determining the suitability of steel in various applications, it is imperative that appropriate alloys are added to steel to ensure that the desired microstructures and therefore properties are exhibited. As such, the effects of steel chemical composition and microstructure, the two key factors, on mechanical properties has been significantly studied in material science and engineering practices. In fact, studies have shown that a material's chemical composition, along with its heat treatment conditions, impact its microstructure [4].

2.2.1 Effects of Chemical Compositions on Mechanical Properties

There are many advantages of adding various alloys to steel to augment its characteristics and behaviors. In general, the addition of copper and nickel to steel has shown to improve corrosion resistance in the alloy; the addition of manganese, silicon, nickel, and copper has improved steel's strength; molybdenum improves hardenability and the addition of calcium, cerium, and zirconium have all shown to improve the alloy's toughness [1], [5]. This is further illustrated by studies that show how modifying chemical compositions independently in a steel mixture through the addition or reduction of specific alloying elements enhances steel's mechanical properties. For example, in the study carried out to determine how annealing temperatures influence mechanical properties and microstructure of high manganese austenitic steels, Yuan et al. [6] proved that carbon and manganese contents play an important role in the improvement of steel's toughness, tensile properties and wear resistance. Generally, carbon and manganese influence the mechanical properties of high manganese steels [7]. Moreover, Gürol et al. [8] showed that increasing a steel's carbon content decreased its impact toughness by increasing the proportion of carbide in the metal. In other words, decreasing carbon content shows toughness and weldability improvements [8], [9]. Furthermore, increasing carbon and manganese contents also increased the hardness and Yield Strength (YS) of the metal due to the carbide precipitation and solid solution strengthening that occurs because of their presence [8]. Lastly, the addition of manganese in steels showed an increase the Ultimate Tensile Strength (UTS) and wear resistance of a steel according to Torabi et al. [10].

Combining various alloying elements has also resulted in unique effects on mechanical properties. In a study examining the effects of composition, specifically the addition of chromium and boron, and the Thermomechanical Controlled Processing (TMCP) on the structure and ageing characteristics of cooper bearing High Strength Low Alloy (HSLA) steels, Banerjee et al. [9] found that a combination of boron and chromium was essential in creating steels with high UTS and YS. Alternatively, samples that contained only boron typically resulted in lower UTS and YS. Additionally, the hardenability of steels was found to be influenced by boron composition along with the addition of other alloying elements. Lastly, the addition of copper to steels with boron and chromium contents showed improved strength and "weld-heat zone-cracking resistance" which reduced or eliminated the requirement of welding preheat. Ultimately, these results showed that combining various alloying elements positively augmented steels depending on the desired properties.

2.2.2 Effects of Microstructure on Mechanical Properties

The microstructural characteristics of steel, including the size and distribution of the grain, and the type of microstructure present, such as martensite or bainite, play a significant role in determining the mechanical properties it exhibits. For instance, grain size impacts the strength and toughness of steel with finer grain having higher strength and toughness, while the presence of different microstructure also affects these properties. One of the main elements that affects a material's microstructure is its TMP.

2.2.2.1 Effects of TMP on Microstructure and Mechanical Properties

TMP, a process that involves simultaneously applying heat and mechanical deformations to a material, significantly affects a steels microstructure. Conditions such as the austenitizing temperature, cooling rate, holding time, deformation, tempering temperatures, and tempering times, all affect the type of microstructures, and their changes, that are present in steel. As such, since microstructures are closely related to the mechanical properties a steel exhibits, it is imperative to study its effects. In a study investigating the structural and phase transformations during the continuous cooling of railroad wheels, Kushnarev et al. [11] found that an intermediate mechanism resulted in the formation of bainitic structures when exposed to cooling rates between 10 and 60 °C/s. This study also found that martensitic structures formed when cooling rates were increased up to 90 °C/s.

Similar findings were found in a study that examined the effects of cooling rate on a low carbon, low alloyed steel microstructure and mechanical properties. Performing tests on thick plates, Wang et al. [12] found that the rate of cooling a metal is exposed to greatly affected its hardness. As the cooling rate increased from 0.5 K/s to 10 K/s, hardness increased correspondingly by a factor of two due to a decrease in soft ferrite. Furthermore, when the cooling rate reached 90 K/s, the reported hardness was nearly three times higher compared to that of a steel cooled at a rate of 0.5 K/s. This increase was attributed to the increase of degenerated upper bainite structures that formed during the TMP. Alternatively, when cooling rates were slower, between 0.5 to 1 K/s, the final microstructure consisted of ferrite with degenerated pearlite and upper bainite resulting in a decrease in hardness.

However, when these rates were increased to 5 K/s or more, the final microstructure consisted only of degenerated upper bainite resulting in an increase in the overall hardness.

Overall, ferrite-pearlite microstructures, which are softer, are present in samples that are slow cooled. These slower cooling rates result in lower hardness values. As the cooling rates increase, these microstructures decrease or change shape resulting in increased hardness. Bainitic phase, which occur at rates near 10 °C, and martensitic formation form with further rate increases which led to even higher hardness results [13]. Ultimately, regardless of the samples thickness, an increase in the cooling rate also increased YS, UTS, and hardness.

2.3 Mechanical Property Prediction using Machine Learning

Due to the availability of large datasets from years of collection, the training of algorithms to predict properties of steel is emerging in research. By obtaining this data, which is typically empirical data from text or through experimentation, robust machine learning models can be used to learn patterns and relationships from complex non-linear variables (inputs) allowing for accurate predictions.

Recently, numerous studies have focused on the use of various machine learning techniques to predict the mechanical properties of steel. For example, Ganguly et al. [14] supplement the development of their genetic algorithm for the optimization of strength and ductility in low carbon steels by implementing an Artificial Neural Network (ANN) to generate the objective functions used in their research. Through this, they found that these NNs could develop objective functions used in solving non-linear optimization problems with multiple variables. Moreover, Das et al. [15] explored the use of statistical and NN

models to explore the non-linearity in empirical modeling of a steel system. In their research, the developed models looked at the relationship between the physical properties of the metal, and its chemistry and rolling parameters. From that, they found that statistical models, especially linear regression models did not accurately predict suitable properties and compositions of metals as those characteristics were complex and non-linear. Although stepwise regression and projection pursuit regression models were better at these predictions, the use of ANNs, especially ones with back propagations, produced the best prediction capabilities. Put simply, ANNs were beneficial as they were able to fit non-linear, difficult data without making assumptions of the properties or distributions of input data. These findings were echoed by Patra et al. and Sidhu et al. [16], [17]. In Patra's work, a neural-network-biased genetic algorithm was proposed for material design. From this, they found that with a large pre-existing dataset, ANNs were beneficial in material design due to their ability to build non-linear heuristic models from the relationships between input and output variables. Sidhu on the other hand focused on the development and experimental validation of a NN model used for the prediction and analysis of the strength of bainitic steels. In this work, it was found that ANNs could be used to accurately predict hardness and therefore strength in these steels, while using inputs from a small database.

Overall, these studies demonstrated that using machine learning, specifically ANNs, has the great potential in predicting mechanical properties in steel and as such illustrate the importance of using computational techniques to optimize the design of new steels.

2.4 Genetic Algorithms Overview

Used in a wide range of engineering and scientific applications, GAs are an optimization technique that mimic the process of natural evolution to find optimal solutions. Based on Darwin's theory of evolution and his principles on survival of the fittest, this search method finds optimal solutions by altering populations using procedures that include reproduction crossovers and mutations [18].

Over the past few decades, research has used GAs in a variety of applications such as machine learning and optimization applications. As an adaptive search method, that can trace the genetic variation within a population of individuals [19], [20], these algorithms are typically domain independent search methods that do not require a priori knowledge about the search space [19]. They operate in a "highly-parallel" manner by finding, enhancing, and reassembling solution components to find the optimal solution to a problem [20]. Although there is no guarantee that GAs are capable of only finding global optimum solutions for a given problem, they typically find an acceptable solution quickly. Furthermore, due to their robustness, parameter setting is not critical, and solutions can be found even when provided with wide margins [2].

As pointed out by Adeli et al. [3], GAs have emerged as an attractive optimization technique for solving problems with large search spaces. This is due to three fundamental features that make them appealing. These are: first, the guarantee of fast convergence to optimal or near optimal solutions due to a group of different starting points, i.e., the pupils; second, they require simple operations to evaluate the functions; and third, they allow for faster computing due to concurrent computing since each variable in the pupils is

independent of each other. The features, among others, make them capable of handling complex search spaces with a high degree of efficiency.

In the field of steel optimization, the use of GAs has gained prominence as a tool to select appropriate chemical composition and heat treatment condition parameters. These optimization problems often involve the evaluation of multiple objectives, such as mechanical properties and cost. In such cases, the use of GAs has shown favourable results highlighting their potential in the development of new steel materials. In the subsequent sections, studies that implements a GA for steel applications will be reviewed and their contributions and limitations shall be discussed.

2.4.1 Application of Genetic Algorithms in Steel Optimization

Various studies utilizing GAs in steel optimization problems have been carried out in recent years due to their ability to handle complex, multi-objective problems. These studies have targeted multiple aspects of steel design focussing on improving material properties such as strength, toughness, and corrosion resistance while minimizing overall cost. In fact, not only can they be used in a variety of applications such as in the atomistic material design, powder compaction, metal rolling, cutting, and welding of steel, they are also used in the development of new material for specified applications [21].

A major area of steel optimization that has immensely implemented the use of GAs is alloy design. In this approach, a GA is used to search for the optimal chemical composition, i.e., alloying element composition, that will produce target mechanical properties of steel. In research carried out by Ganguly et al. [14] the use of GAs in the optimization of strength and ductility in low carbon steels was proposed. Through this

study, it was found that GAs could successfully manipulate a potential steel's alloying element composition to meet specified targets efficiently and accurately. This was echoed in research carried out by Mahfouf et al. [22]. In the optimal design of alloy steels, the authors used a multi-objective optimization GA to predict the chemical compositions also successfully meeting their target mechanical properties – tensile strength, reduction area, and elongation.

Another area that GAs are used for steel optimization is in the optimization of heat processing treatment. In this area, the GA is used to determine the optimal heat treatment conditions that will result in desired mechanical properties of steel. For example, Srinivasan et al. [23] utilized GAs in the optimal design of high carbon bainitic steels by concurrently optimizing the alloying elements and the heat treatment parameters. This approach was also taken by Ganguly et al. [14]. In their approach, deformation above and below recrystallization temperatures, cooling rates, slab reheating temperatures and finish rolling temperatures, were used in conjunction with chemical compositions to determine suitable configurations that optimize for strength and ductility in low carbon steels. In both these applications, it was found that GAs could find accurate solutions in the complicated optimization problem.

Lastly, GAs have also been used in microstructure optimization. In this area of steel optimization, they determine optimal microstructures that a steel needs to meet target mechanical properties. Chua et al. [24] for example, used this approach to predict the complex structure of interfaces found in multicomponent systems, specifically $SrTiO_3$, a complex oxide. Unlike in traditional searches where the optimization target is to meet a

global minimum, the authors opted to bias their GA away from this minimum. Nonetheless, it was demonstrated that GAs can be used to accurately determine the complex structures of interfaces of multicomponent systems.

Overall, the application of GAs in steel optimization has shown improvements in mechanical properties of steel while minimizing cost and the studies highlighted in this section demonstrate this.

2.4.2 Comparison of Genetic Algorithms with Other Optimization Techniques

Although GAs have been successful in optimizing multiple objectives for target mechanical properties and cost, hence their popularity, there are numerous other optimization techniques available that can also solve steel optimization problems. These techniques include NNs, random search methods, gradient search methods, iterative search methods, and simulated annealing. All these methods have their advantages and disadvantages; as such, it is important to compare these techniques to determine their effectiveness in comparison to the use of GAs.

One example of an optimization technique that has notably been used for steel optimization is the NN method with Fuzzy logic being the most common type. First explored by Zadeh in Fuzzy Sets [25], the use of fuzzy set theory showed that it could deal with imprecise data that contained large uncertainties. This allowed for optimization algorithms to find the true optimal solution as they were not constrained to targets with small tolerances [3]. Due to this ability, it was found that fuzzy logic was beneficial for problems that involved structural loads. Although it was found to be a useful tool, there are several factors that make it inadequate for use for a material property and cost optimization

problem. The main one being the sensitivity to noise that may be present in the input data. This is a main disadvantage since real word data is usually noisy.

Another example of an optimization technique that is used in steel optimization is Simulated Annealing (SA). A stochastic optimization technique, SA iteratively adjusts input parameters by randomly selecting parameters, calculating the objective function, and accepting results that lead to improvement in that function. This approach has been shown to be beneficial in large search spaces when the objective function is non-linear and non-differentiable. With that being said, Chakraborti et al. [21] found that GAs ultimately performed better than the traditional SA methods.

Alternatively, Dulikravich et al. [26] explored the use of an Indirect Optimization based upon Self-Organization (IOSO) algorithm to select alloying elements in the optimization of a few mechanical properties. In this work, the authors showed that this methodology was highly reliable as it was able to avoid local minimums. Further, it could accomplish this with faster computing times, and with a small dataset. In fact, this methodology was selected over more popular methodologies such as the use of NNs since they found that the use of ANNs alone were not reliable for developing search algorithms in optimization problems as that was not their originally intended design leading to inefficient and inaccurate results.

Overall, while there are numerous optimization techniques available for steel optimization, each one has its own advantages and limitations. GAs and NNs approaches for instance are robust and flexible methods that can deal with non-linear and noisy data making them the optimal solution for most application specific problems [2]. Moreover,

they are typically capable of evaluating designs with discrete and continuous variables [3]. Random search methods on the other hand, are inefficient as they take a brute force approach to finding solutions and gradient methods are ineffective in multi-modal functions where the local maximum will be selected as the optimal solution. Lastly, iterated and simulated annealing search methods, although simple, tend to overlook the overall pictures of the search space [2]. Ultimately, the choice of the technique to use depends on the application, however, through comparison of the different methods for the steel optimization problem, the use of GAs has proven to be the most efficient and accurate.

2.4.3 Advantages and Limitations of using Genetic Algorithms in Steel Optimization

As an optimization technique, GAs have their own sets of advantages and limitations that must be considered to ensure that they are effective for steel optimization. One of the significant advantages of using GAs is its ability to handle complex, non-linear optimization problems. Moreover, they are robust and flexible allowing for fast convergence even with simple operations to evaluate the objective function [2], [3]. These characteristics are beneficial for multi-variable, multi-objective problems making them suitable for steel optimization. For the case of the optimization of mechanical properties such as strength, ductility and toughness, GAs can evaluate targets with multiple parameter inputs such as chemical composition and heat treatment conditions.

However, GAs have some limitations depending on the application. The main limitation being that the GAs success depends on the diversity of the initial population. This means that if this population is not diverse, suboptimal solutions may dominate the generated populations causing a convergence to a local minimum. This would ultimately

result in incorrect solutions [2], [3]. The main reason this occurs is due to the improper selection crossover and mutation parameters when finding a solution. Lastly, GAs typically require many evaluations to find the optimal. This is not feasible during some optimization applications due to cost and time restrictions.

Overall, there are several advantages for the use of GAs in steel optimization. The main advantage of using this method is its ability to handle complex discrete or continuous data, with multiple specified targets. However, they also have limitations such as a tendency to incorrectly select local optima when improper starting parameters are selected. Ultimately, considering these advantages and limitations is imperative in effectively using these algorithms for steel optimization.

Chapter 3 Methodology

3.1 Problem Formulation

The problem formulated in this research is an unconstrained optimization problem defined by the objective function with a penalty term for the target material properties. The objective function, which is the subject to be minimized, is the manufacturing cost (MC). Initially formulated as the constrained optimization problem MC: $X \subset \mathbb{R}^m$ constrained to $g(x) = 0$ for $m = 3$ where, X represents the input parameters i.e., alloying elements, and the 8 points (time and temperature) from the cooling profiles, and m represents the number of target mechanical properties (HV, TS, and TE). The equivalent unconstrained problem is shown in Equation (1) as proposed by Tanner and Srinivasan [27].

$$\min_{x \in X} f(x; \varsigma) = \min_{x \in X} [s(x) + \varsigma g(x)^{\mathrm{T}} D g(s)] \quad (1)$$

In this equation, $g^T D g$ is the introduced penalty term used to reformulate the constrained problem. D is a diagonal positive definite matrix, and T represents a transpose. $\varsigma > 0$ is a penalty parameter such that if $x^* = \min_{x \in X} f(x; \varsigma)$ then $\lim_{x \to \infty} x_\varsigma^* = x^*$. The original solution to the constrained optimization problem is x^*, and the solution to the unconstrained optimization is x_ς^*. This means that a solution x_ς^* close to the optimum x^* depends on the choice of the penalty term, ς.

3.2 Objective Cost Function

The objective cost function *(f)* used for the analysis is based on the formulation that was proposed by Srinivasan et al. and Tanner and Srinivasan [23], [27] and is summarized

in Equation (2). This formulation consists of the MC, which comprises of the cost of the alloying elements and the energy required for TMP (shown in Appendix C), and the penalty term which is represented by three mechanical properties – hardness (HV), tensile strength (TS), and tensile elongation (TE). This function is formulated as follows:

$$f(x,\varsigma) = \frac{Co}{2}\left(\frac{MC}{MC_0}\right)^{co} + \frac{\varsigma}{2}\left[H\left|\frac{HV - HV_0}{HV_0}\right|^{h} + S\left|\frac{TS - TS_0}{TS_0}\right|^{s} + E\left|\frac{TE - TE_0}{TE_0}\right|^{e}\right] \quad (2)$$

Where, x represents the input parameters, ς the penalty parameters, Co, H, S, and E, are the positive weights, and co, h, s, and e, are the positive exponents. The weights and exponents are used to determine each term's importance. Lastly, the target values are denoted by the 0 subscripts.

Different cost function formulations were explored to analyze the functionality of the developed optimization algorithm. This was accomplished by varying the weights and exponents in the formula giving preference to specific variables and therefore targets. According to Srinivasan et al. [23], the dependence between the outputs and the material properties, HV, TS, and TE, are not known and therefore an iterative process is required to search the parameters and update the penalty parameter. Updating the penalty parameters uses the formulation outlined by Srinivasan et al. [23] and is shown in Equation (3).

$$\varsigma^{k+1} = \frac{Co\left(\frac{MC^k}{MC_0}\right)^{co}}{H\left|\frac{HV^k - HV_0}{HV_0}\right|^{h} + S\left|\frac{TS^k - TS_0}{TS_0}\right|^{s} + E\left|\frac{TE^k - TE_0}{TE_0}\right|^{e}} \quad (3)$$

$$\varsigma^{k+1} = \max\left(\varsigma^{k}, \varsigma^{k+1}\right) \quad (4)$$

k and *k+1* are the values from the current and next iterations during the solving process. During this process, the maximum of the two is selected for the next iteration as shown in Equation (4). This gives the penalty parameters more weights as the iteration continue thus constraining the optimization parameter, MC, to a minimum.

3.3 Development of Reduced Order Models

To predicts a steel's mechanical properties, ROMs were developed. These models aimed at predicting these mechanical properties based on certain input parameters. To accomplish this, NN or correlation equations were used to develop these models. In this research, three ROMs were considered and are:

(1) Reduced Order Hardness (ROH) model

(2) Tensile Strength Model

(3) Elongation Model

These models are summarized below.

3.3.1 Hardness Model

A Multilayer Perceptron (MLP) ANN model was used to develop the ROH model for the hardness prediction within the μGA due to its ability to solve non-linear problems [14]. This model consisted of an input layer with 33 inputs, 2 hidden layers containing 64 neurons each, and an output layer for hardness prediction as illustrated by Figure 3-1. The model was trained using the selected input parameters namely; the average cooling rates, austenitizing temperatures, 8 points from a cooling profile, chemical compositions, and hardness values retrieved from the ATLAS [28]. Table 3-1 summarizes these input parameters. This model is represented by Equation (5)

where, n is the number of inputs (33), m is the number of neurons in each hidden layer (64), x is the input, w is the coefficients, b is the bias, and a is the activation function represented by the ReLU function, $a = \max(0, x_i)$. Additional details on the model's hyperparameters and testing results can be found in Appendix A.

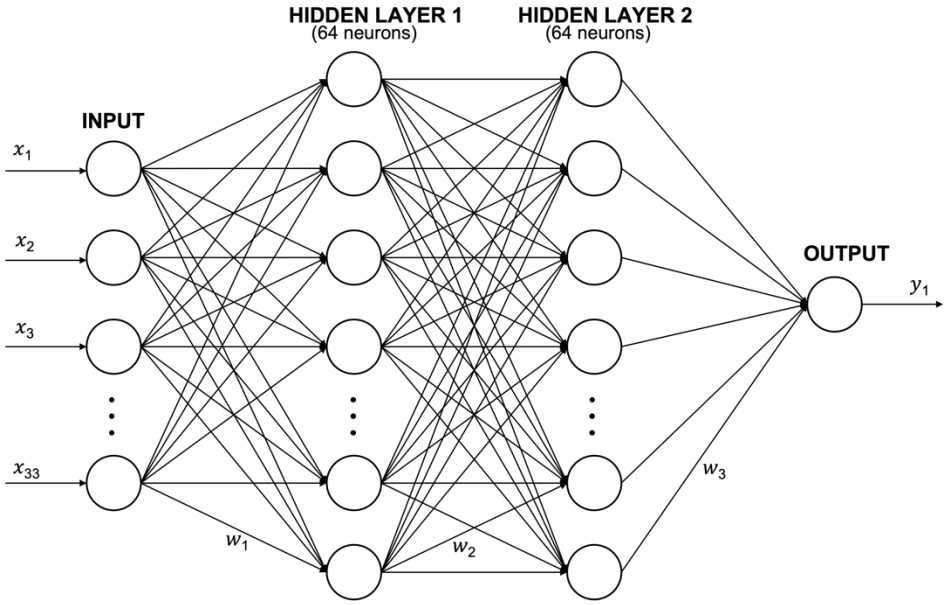

Figure 3-1: Reduced Order Hardness Model Neural Network Schematic

$$HV = a\left(\sum_{i=1}^{n} w_i^{(3)}\left(a\left(\sum_{i=1}^{m} w_i^{(2)}\left(a\left(\sum_{i=1}^{m} w_i^{(1)}x_i + b^{(1)}\right)\right) + b^{(2)}\right)\right) + b^{(3)}\right) \quad (5)$$

3.3.2 Tensile Strength Model

The tensile strength model was obtained using the correlation equation developed by Pavlina et al. [29]. This equation outlined in Equation (6).

$$TS = 3.734 \times HV - 99.8 \quad (6)$$

3.3.3 Elongation Model

The elongation model was similarly calculated using the correlation equation obtained from data reported by Bhattacharya [30] and Matlock [31] shown in Figure 3-2. The extracted points are shown in Figure 3-3 and the correlation equation is summarized by the Equation (7).

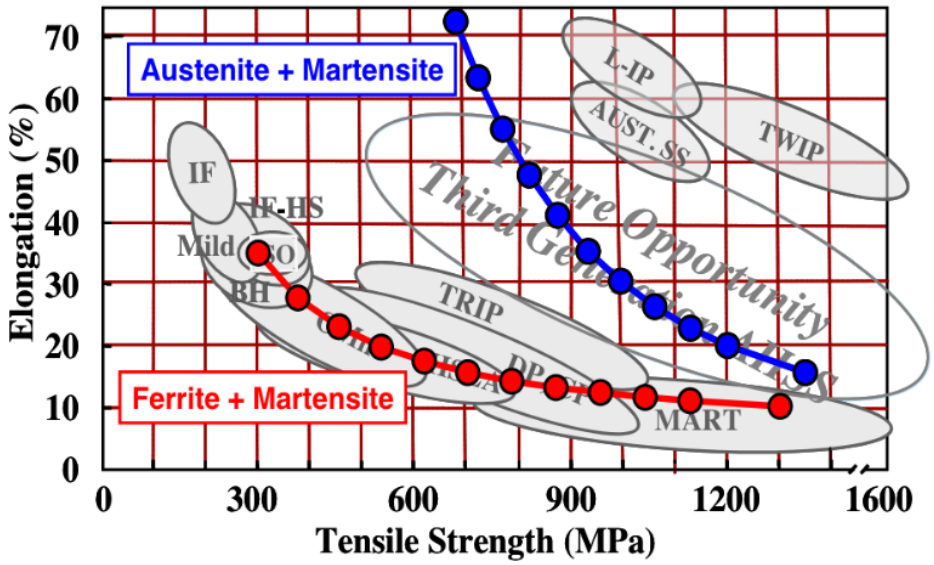

Figure 3-2: Elongation as a function of Tensile Strength used to Develop the Correlation Equation as Extracted from Bhattacharya [30]

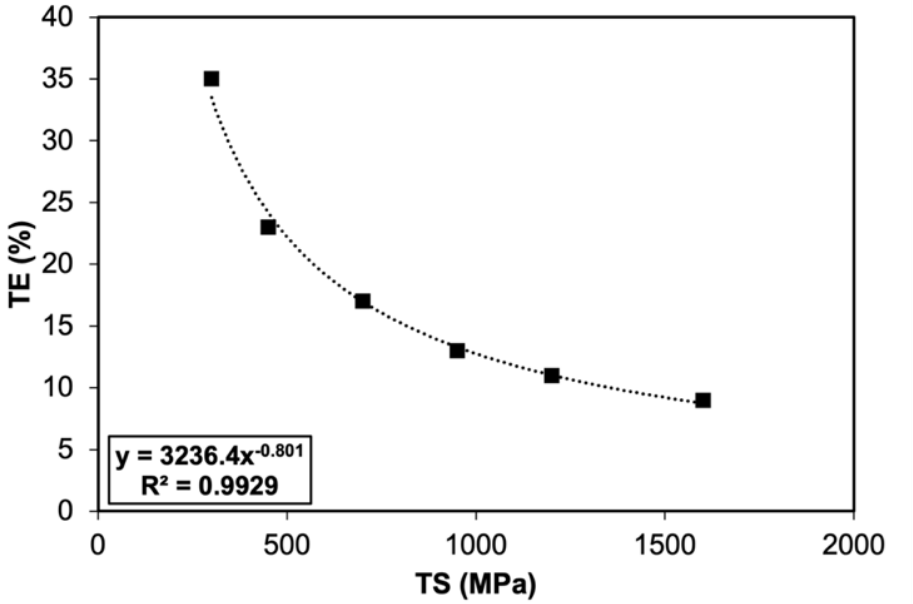

Figure 3-3: Correlation between Tensile Strength (TS) and Elongation (TE) as Extracted from Data Reported by Bhattacharya [30]

$$TE = 3236.4 \times TS^{-0.801} \quad (7)$$

3.4 Genetic Algorithms Optimization Solver

A μGA, which is a subset of the traditional GA, was chosen as the optimization solver in this research. This was done to improve the overall optimization process because, μGAs have the advantage of being able to converge quickly and efficiently – similar to the traditional GAs [2], [18], [20], [23] – but with the added benefit of needing fewer iterations and smaller population sizes [23]. Therefore, they were selected as the optimization method to effectively optimize the steel parameters required to meet specified material property and cost targets.

A μGA is predominately made up of two elements – populations and pupils – and it undergoes a series of iterations or generations to find the optimal target. In this case, a

pupil represents the input parameters, and a population represents the number of pupils in each generation. The pupils were represented by the 33 inputs that were used to train the ROH and microstructure prediction models. These inputs are the average cooling rate, the austenitizing temperature, 8 points from the cooling profiles, and the alloying element compositions. The range of these parameters is summarized in Table 3-1. Unlike traditional GAs that are typically comprised of approximately 500 – 1000 pupils [19], 5 pupils were selected for the μGA.

Table 3-1: Summary of the Input Parameters Search Space

Parameters	Range
t (s)	$0.10 – 1.88 \times 10^{5}$
T (F)	140 – 1775
T_{aus} (F)	1433 – 1950
CR_{ave} (F/s)	0 – 5153
C (wt. %)	0.10 – 2.19
Mn (wt. %)	0.20 – 1.98
P (wt. %)	0 – 0.44
S (wt. %)	0 – 0.29
Si (wt. %)	0 – 1.05
Ni (wt. %)	0 – 3.03
Cr (wt. %)	0 – 13.12
Mo (wt. %)	0 – 0.56
Cu (wt. %)	0 – 0.91
Al (wt. %)	0 – 0.06
V (wt. %)	0 – 0.31
B (wt. %)	0 – 0.05
N (wt. %)	$0 – 3.00 \times 10^{-3}$
Ti (wt. %)	0 – 0.18
W (wt. %)	0 – 1.15

To determine the optimal solution for a specific target, HV_0, TS_0 and TE_0, the algorithm randomly generated 5 different pupils. These pupils consisted of the input parameters outlined in Table 3-1. The 15 alloying elements were generated within the allocated ranges. A Lagrange polynomial formulation was used in this study to define the cooling profile. The specific quartic polynomial that was employed is given by:

$$T(t) = at^4 + bt^3 + ct^2 + dt + e \quad (8)$$

where T is the temperature, t is the time, and a, b, c, d, and e, are the calculated coefficients or constants. To obtain these coefficients or constants and generate a new cooling profile for each pupil, the algorithm generated an initial set of 5 time-temperature input combinations within the specified range, with increasing time and decreasing temperatures. These values were used to construct a quartic Lagrange interpolating polynomial from the following form: $L(t) = \sum_{j=0}^{k} T_j l_j(t)$, where L is the interpolating polynomial, j is the index, k is the total number of nodes (4 for quartic), and l is the basis polynomial. The remaining 3 time-inputs were then selected to lie between the other points on the curve and the corresponding temperatures calculated from the profile's equation ensuring that the resulting polynomial function provided a smooth and continuous representation of the cooling profile. This process was repeated for every pupil generation, ensuring that each new generation had its own unique cooling profile.

The manufacturing cost of each pupil was calculated and their corresponding HV, TS, and TE, predicted. The fitness of these pupils was evaluated using the cost function outlined in Equation (1). Once the cost function was evaluated, the penalty parameter for the next iteration was determined. This new parameter was calculated as per Equations (3), and (4). In the first iteration, a start penalty of 1×10^2 was arbitrarily assigned for each pupil. Moving into the next iterations, the pupil that generated the minimum cost function was kept, and the remaining 4 pupils discarded prior to the start of the next iterations. In the new iterations, 4 new pupils were generated and along with the best pupil of the previous iteration, the evaluation was repeated. This was done for 2500 iterations. Figure

3-4 illustrates the developed algorithm's procedure. Appendix B shows the corresponding pseudo code.

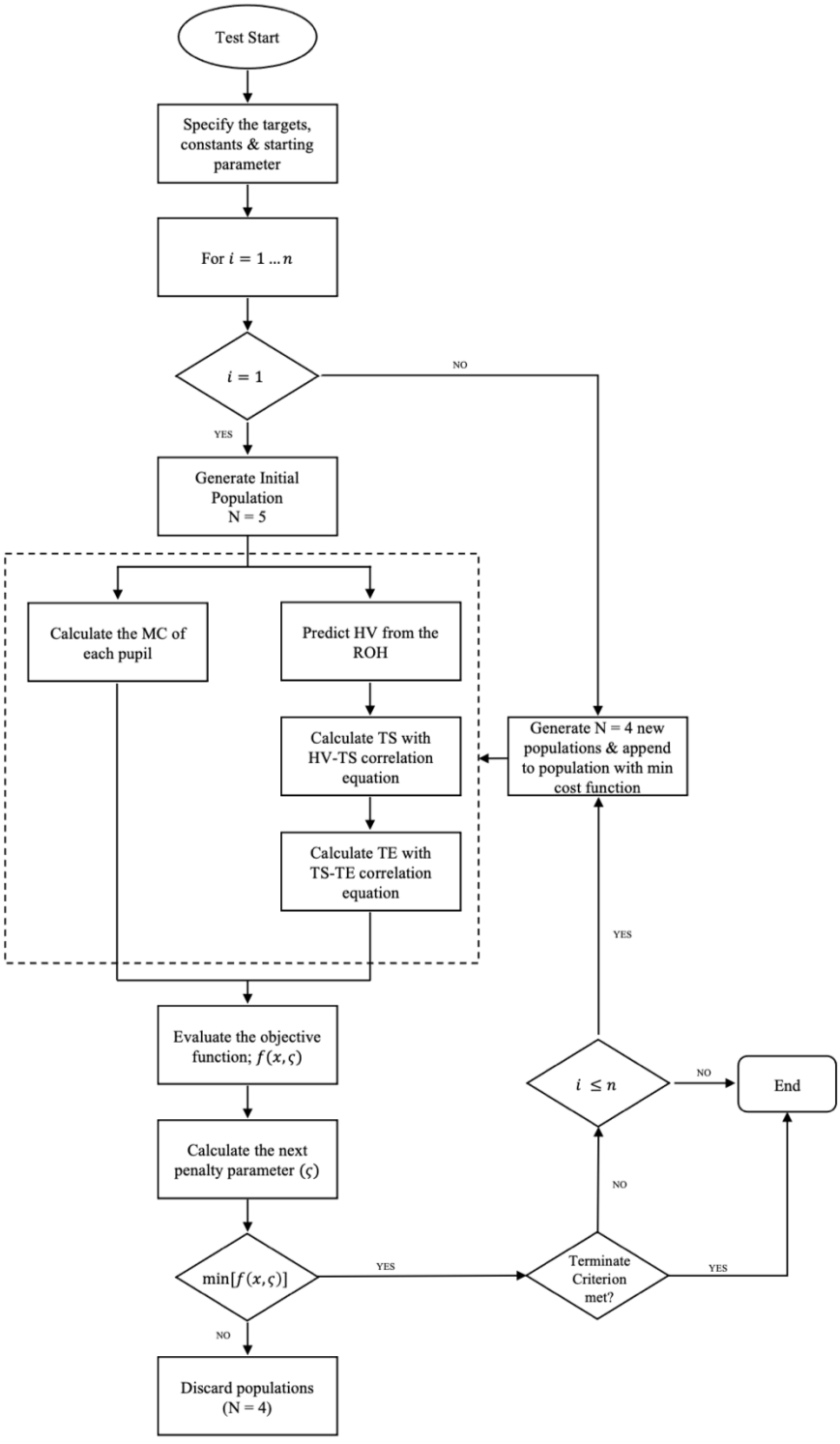

Figure 3-4: Illustration of the μGA's Procedure

3.5 Computational Cases

The computation cases summarized in Table 3-2 were developed to test the algorithm's ability to find the optimal solution that meets the required targets while minimizing the cost by evaluating the cost function equation. To accomplish this, a baseline and six different cases were considered in this study.

In the baseline case, all constants (weights and exponents) in Equation (2) were set to 1. For the remaining cases, specific constants were set to an arbitrary value of 10 to change the impact each target has during the search process. For example, in Case H1, the weight H was set to 10, and the rest of the constants were 1. Alternatively, for Case H2, the exponents s, and e, were set to 10 and the rest of the constants were set to 1. By increasing specific exponent values, their corresponding properties are deemphasized. Consequently, increasing a specific weight emphasized its corresponding property. For example, in Case T2, an increase of h, and e, by 10 deemphasized the hardness and elongation properties thus emphasized tensile strength. Similarly, increasing T by 10 in Case T1, also emphasized tensile strength but without drastically deemphasizing hardness and elongation.

For each of the computation cases, the algorithm was set to terminate after 2500 generations, which is the maximum number of generations allowed in the study. The termination criterion was set such that each run would stop if a steel with a cost lower than \$0.05/100g was generated.

Table 3-2: Summary of the Values of the Weights and Exponents used in Equation (2) for the Different Cases

Case	Weight Constants			Exponent Constants		
	H	**S**	**E**	**h**	**s**	**e**
Baseline	1	1	1	1	1	1
H1	10	1	1	1	1	1
H2	1	1	1	1	10	10
S1	1	10	1	1	1	1
S2	1	1	1	10	1	10
E1	1	1	10	1	1	1
E2	1	1	1	10	10	1

Chapter 4 Results and Discussions

4.1 Methodology Validation

To validate the methodology of the developed μGA two methods were used. These included a developed microstructure prediction model and the validation of the GA using standard functions. The microstructure model was used to assess whether the generated population yield suitable microstructure based on literature. Validating the genetic algorithm with standard functions evaluated its capability to generate results that were accurate. The subsections below provide further detail on these two methods.

4.1.1 Microstructure Prediction Model

A NN model that predicts a steel's microstructure based on alloying elements and heat treatment conditions was developed. This model served as secondary approach to validate whether the generated population from the optimization algorithm yielded reasonable outcomes. This was accomplished by comparing the predicted microstructure with expected theoretical outcomes outlined in literature. For example, ferrite-pearlite microstructures are typically present in samples that are slow cooled [13]; therefore, if the resulting population had heat treatments conditions exhibiting slow cooled behaviors, they will most likely contain such microstructures. Alternatively, degenerated upper bainite final structures are expected in samples treated with higher cooling rates while quenched and tempered steels typically comprise of tempered martensitic structures [11], [12], [32].

Like the ROH model, the designed NN for this prediction model is an MLP that takes 33 inputs in the input layer. These inputs correspond to the average cooling rates,

austenitizing temperatures, chemical compositions, and 8 points from the Time-Temperature-Transformation (TTT) diagrams. It also contains 2 hidden layers with 10 and 5 neurons respectively, and an output layer with 5 outputs. These outputs are the austenite, ferrite, pearlite, bainite and martensite percentages. The developed model is illustrated in Figure 4-1. Further information on the model's hyperparameters and testing results are shown in Appendix A.

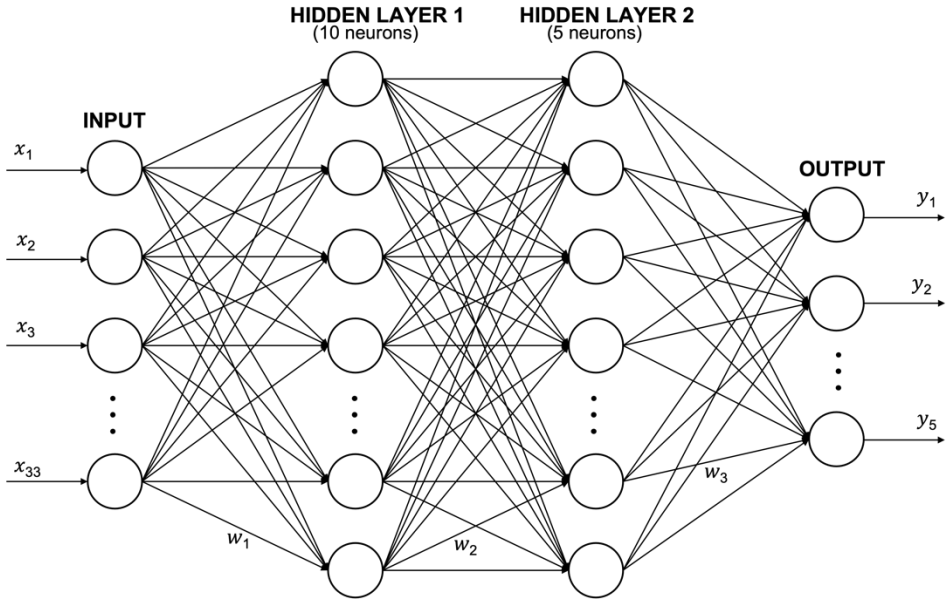

Figure 4-1: Microstructure prediction Model Neural Network Schematic

4.1.2 Genetic Algorithm Validation

To evaluate the effectiveness of the designed μGA, which has no mutations and utilizes fewer iterations and a smaller population size, its performance was tested against three standard test functions within the two-dimensional search space. The considered testing algorithms, their formulations, illustrations (Figure 4-2), and their results are summarized below.

1) McCormick Function

$$f(x,y) = \sin(x+y) + (x-y)^2 - 1.5x + 2.5y + 1 \quad (9)$$

Where $x \in [-1.5,4]$ and $y \in [-3,4]$

2) Easom Function

$$f(x,y) = -\cos(x)\cos(y)\exp(-(x-\pi)^2 - (y-\pi)^2) \quad (10)$$

Where $x \in [-100,100]$ and $y \in [-100,100]$

3) Ackley Function

$$f(x,y) = -20\exp\left(-0.2\sqrt{\frac{1}{2}(x^2+y^2)}\right) - \exp\left(\frac{1}{2}(cos(2\pi x) + cos(2\pi y))\right) + 20 + \exp(1) \quad (11)$$

Where $x \in [-32.8,32.8]$ and $y \in [-32.8,32.8]$

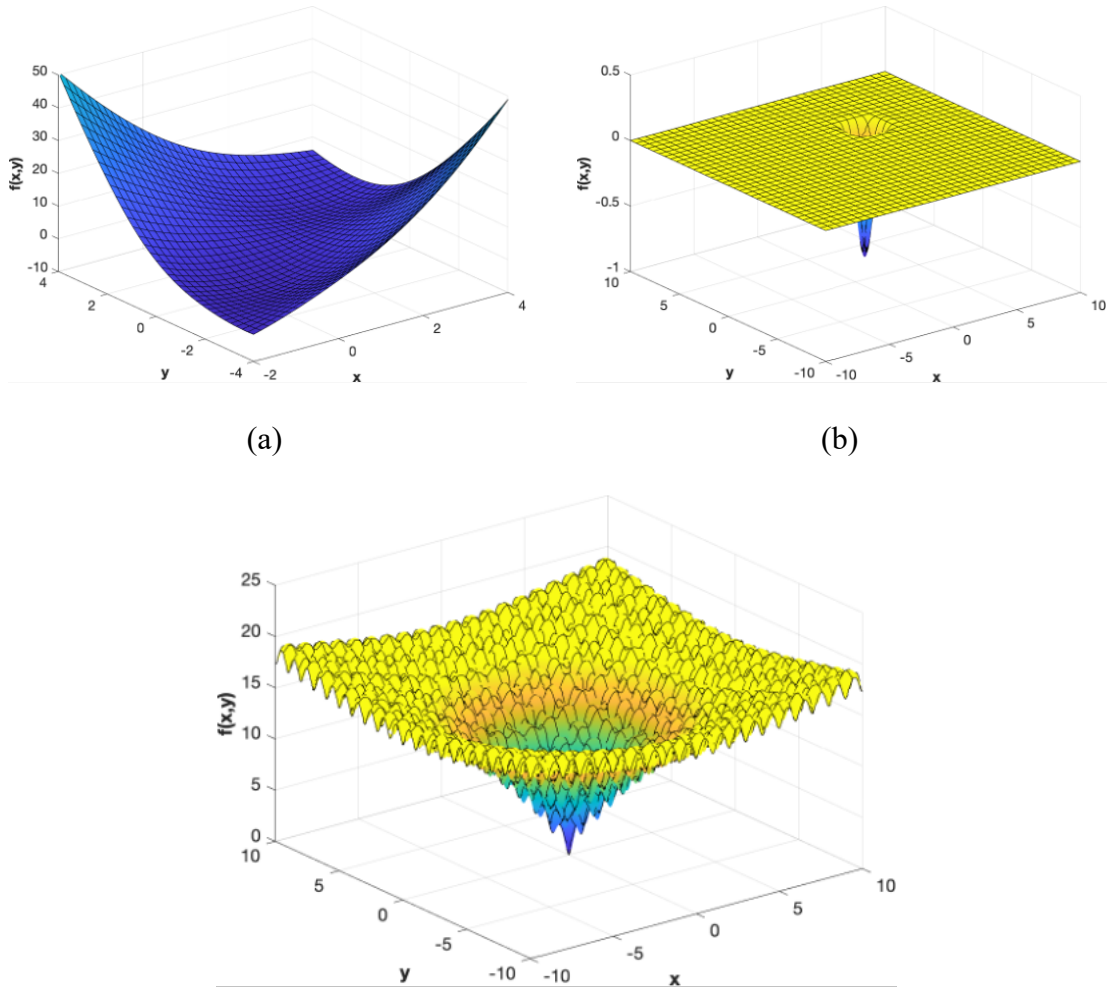

Figure 4-2: Standard Test Functions used to Test the μGA's Performance. (a) McCormick Standard Test Function [33], (b) Easom Standard Test Function [34], (c) Ackley Standard Test Function [35]

McCormick, Easom, and Ackley's functions were selected due to their diverse topographies and varying degrees of complexity. McCormick's Function, represented by Equation (9) was selected as a simple function to test due to its smooth surface and easy to find global minimum. Further, selecting a function with a more defined, but smooth, minimum, such as Easom's function represented by Equation (10), further reinforced the robustness of the designed algorithm. Lastly, to test its ability to handle a complex search,

the algorithm was also tested with Ackley's Function (Equation (11)) due to its multiple local optimums. It is easy to see from Figure 4-2 that a gradient based algorithm would be able to find the global minimum only if one starts the search very close to the global minimum. Thus, the ability of our algorithm to determine the global optimum in all three cases would establish the validity of the algorithm.

The results of using this algorithm on these functions are summarized in Table 4-1. As shown, the μGA was fairly accurate in predicting the global minimums of all the functions, irrespective of the random starting population. The typical number of function evaluations needed for the three test functions are 111, 1370 and 1345 for the McCormick, Easom and Ackley's functions, respectively. Moreover, the cost for each function was also accurately predicted for all three test functions at a significantly lower number of iterations. With these results, it is safe to conclude that the μGA algorithm proposed in this work is suitable for solving the steel optimization problem.

Table 4-1: μGA Results Tested on Standard Test Functions

Function	**Global Minimum (x, y)**		**Optimal Cost**	
	Theory	μGA	Theory	μGA
McCormick	(-0.54719, -1.54719)	(-0.55506, -1.53218)	- 1.913	-1.9127
Easom	(π, π)	(3.12756, 3.14902)	-1	-0.9996
Ackley	(0, 0)	(0.01086,0.01171)	0	0.0520

4.2 Optimizing for Mechanical Property Results

To optimize for the mechanical properties (hardness, tensile strength, and elongation), three representative steels were chosen to represent low, medium, and high

strength steels. These steels are AISI 8620, 4130, and 420 Stainless Steel respectively. Their corresponding properties are shown Table 4-2. The results of the GAs performance based on its ability to meet specified targets are discussed in the subsequent sections.

Table 4-2: Mechanical Properties of Selected Representative Steels used in the Analysis

Steel Name	**Mechanical Properties**		
	Hardness (V)	Tensile Strength (MPa)	Elongation (%)
AISI 8620 Steel	178	565	28.5
AISI 4130 Steel	286	917	19
420 Stainless Steel	525	1705	13.5

4.2.1 Optimization Results for Low Strength Steels

Table 4-3 shows the algorithm results for generated steels with AISI 8620 mechanical property targets for the different computational cases. Table 4-4 shows the corresponding microstructure predictions.

Table 4-3: Algorithm Results for AISI 8620 for the Different Computational Cases

Cases	**Baseline**	**H1**	**H2**	**S1**	**S2**	**E1**	**E2**
Key parameters							
T_{aus} (F)	1521	1636	1742	1520	1552	1552	1788
CRave (F/s)	130	133	122	158	185	191	2
C (wt. %)	0.11	0.40	0.31	0.34	0.14	0.17	0.10
Mn (wt. %)	0.94	0.88	0.30	0.82	0.92	0.36	0.23
P (wt. %)	0.02	0.01	0.03	0.01	0.00	0.02	0.03
S (wt. %)	0.02	0.02	0.01	0.02	0.01	0.01	0.00
Si (wt. %)	0.16	0.17	0.25	0.15	0.22	0.26	0.28
Ni (wt. %)	0.33	0.28	0.36	0.31	0.15	0.35	0.05
Cr (wt. %)	1.00	0.90	0.14	1.42	0.92	0.22	0.10
Mo (wt. %)	0.03	0.03	0.00	0.03	0.01	0.02	0.02
Cu (wt. %)	0.05	0.02	0.25	0.20	0.24	0.13	0.00
Al (wt. %)	0.00	0.00	0.00	0.01	0.00	0.00	0.00
V (wt. %)	0.01	0.01	0.00	0.01	0.01	0.01	0.01
B (wt. %)	0.00	0.00	0.00	0.00	0.00	0.00	0.00
N (wt. %)	0.00	0.00	0.00	0.00	0.00	0.00	0.00
Ti (wt. %)	0.01	0.01	0.01	0.00	0.01	0.00	0.01
W (wt. %)	0.05	0.01	0.05	0.05	0.00	0.06	0.03
Mechanical Properties and Cost							
HV	177.9	178.2	178.0	178.0	178.5	124.8	124.8

Cases	**Baseline**	**H1**	**H2**	**S1**	**S2**	**E1**	**E2**
TS (MPa)	564.5	565.5	564.8	565.0	566.6	366.1	366.2
TE (%)	20.2	20.2	20.2	20.2	20.2	28.6	28.6
Optimal Cost ($/100g)	0.35	0.87	0.20	0.45	0.27	0.23	0.26

Table 4-4: Microstructure Predictions for AISI 8620 for the Different Cases

Cases	**Microstructure (%)**					
	Austenite	Ferrite	Pearlite	Bainite	Martensite	Error
Baseline	0	47	29	16	4	4
H1	0	8	92	0	0	0
H2	0	36	58	3	0	3
S1	0	12	87	0	0	1
S2	0	71	21	2	0	6
E1	0	82	11	1	0	6
E2	0	79	15	0	0	6

For the baseline case, the weights and exponents in the cost objective function are set to 1. In this case, a low alloy, medium carbon content steel was generated from the algorithm. This yielded accuracies of 100% for HV and TS, and 71% for TE. Figure 4-3 (a – c) show the change of these properties over 2500 generations. The values stabilized after 750 iterations allowing for an exhaustive search within the search space. This resulted in

accurate results with an optimized cost of $0.35/100 g. Notably, the generated steel has high manganese and chromium contents. Both these alloys significantly contribute to its hardness [1], [6], [8]–[10], [36]. The corresponding cooling profile for the generated steel is shown in Figure 4-3 (d). Taking over 2000 seconds for the heat treatment process to complete, the steel is slow cooled indicating a likely presence of ferrite-pearlite microstructures [13]. This was proved by utilizing the developed microstructure prediction model. From this model, the microstructure was predicted to consist of mainly ferrite and pearlite with a total percentage of about 76%, and the remainder being bainite and martensite. This is further consistent with results documented in the Classification and Designation of Carbon and Low-Alloy Steels ASM Handbook [37]. The penalty parameter as shown by Figure 4-3 (e) remained unchanged as a high initial penalty was chosen. As expected, the cost function decreased over the iterations as shown in Figure 4-3 (f).

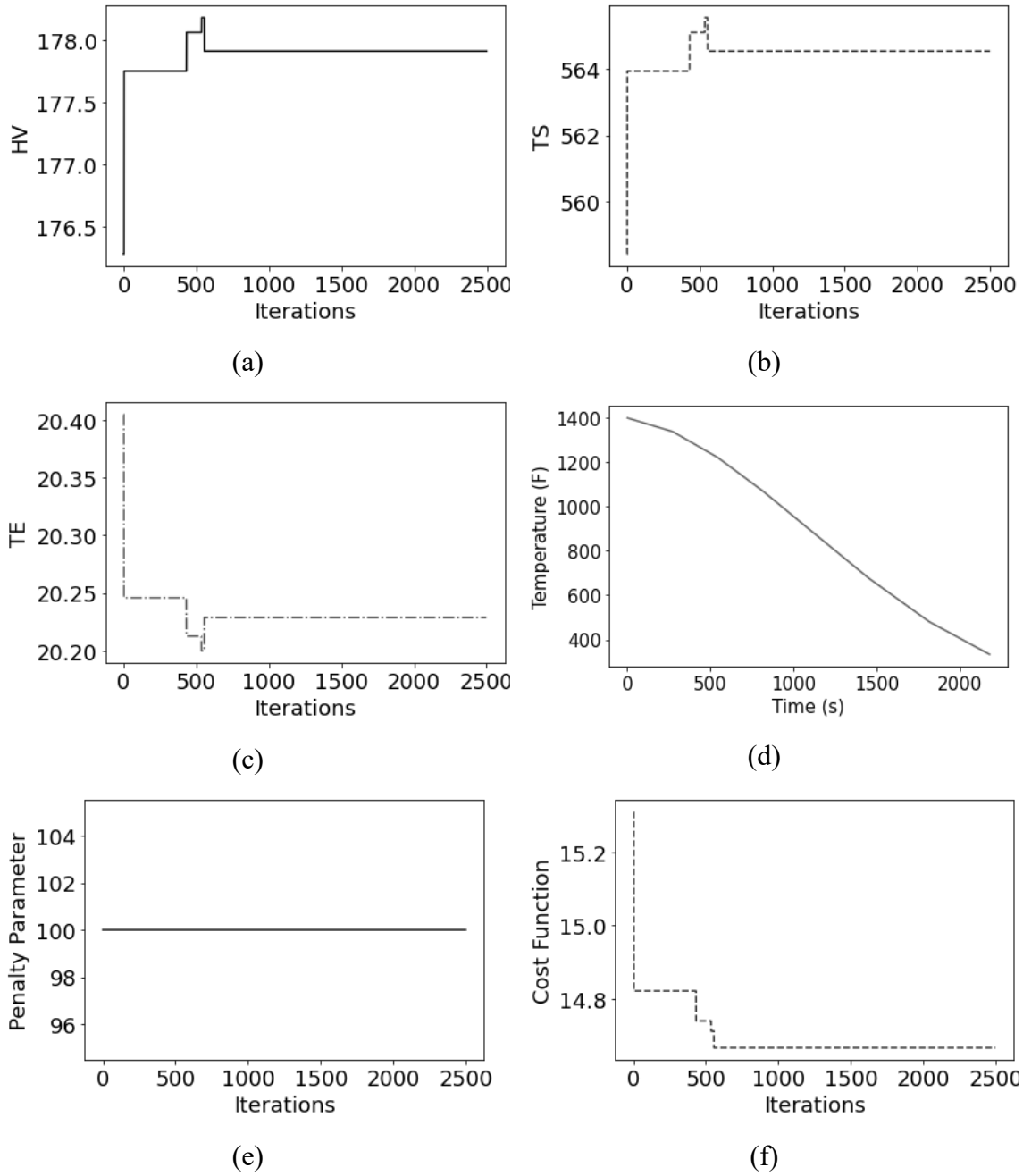

Figure 4-3: Results of the μGA for the Baseline Case for AISI 8620. (a – c) The Mechanical Properties – Hardness, Tensile Strength, Elongation, (d) the Cooling profile, (e) the Penalty Parameter, and (f) the Cost Function

To emphasize for the hardness property, the weight H or the exponents s and e, were raised to a value of 10. For case H1, where the weight H was raised to 10 and the remainder of the weights and exponents remained 1, accuracies of approximately 100% for HV and TS, and 71% were produced like in the baseline case. However, the predicted cost was much higher at $ 0.87 / 100 g. Since the generated compositions were comparable to that of the baseline case except for the carbon content where a low carbon content steel was produced for the baseline and a medium carbon content steel for H1, the main contributor to this significant increase in cost was the heat treatment time. It took more than 20 times longer for this process in the case of H1 in comparison to the baseline case. Due to this slow cooling process, the steels microstructure was made up of ferrite and pearlite as expected.

In the case of H2, where exponents s, and e, were raised by a factor of 10, a medium carbon content steel with manganese and chromium contents lower than in the H1 case was generated. However, its corresponding cooling profile was significantly shorter than that of H1 resulting in cheaper steel alternative. In fact, this generation was the lowest in all cases for the low strength steel trial as the cooling time took less than 60 s. At this higher cooling rate, some bainitic or martensitic microstructures were expected as there is a decrease in the ferrite-pearlite structures [13]. In this case, the steel's microstructure contained ferrite-pearlite structures along with some bainite as expected. Figure 4-4 shows the results of the mechanical properties, penalty parameters and cost function over 2500 generations for both cases, H1 and H2, and Figure 4-7 (a, b) shows the corresponding cooling profiles.

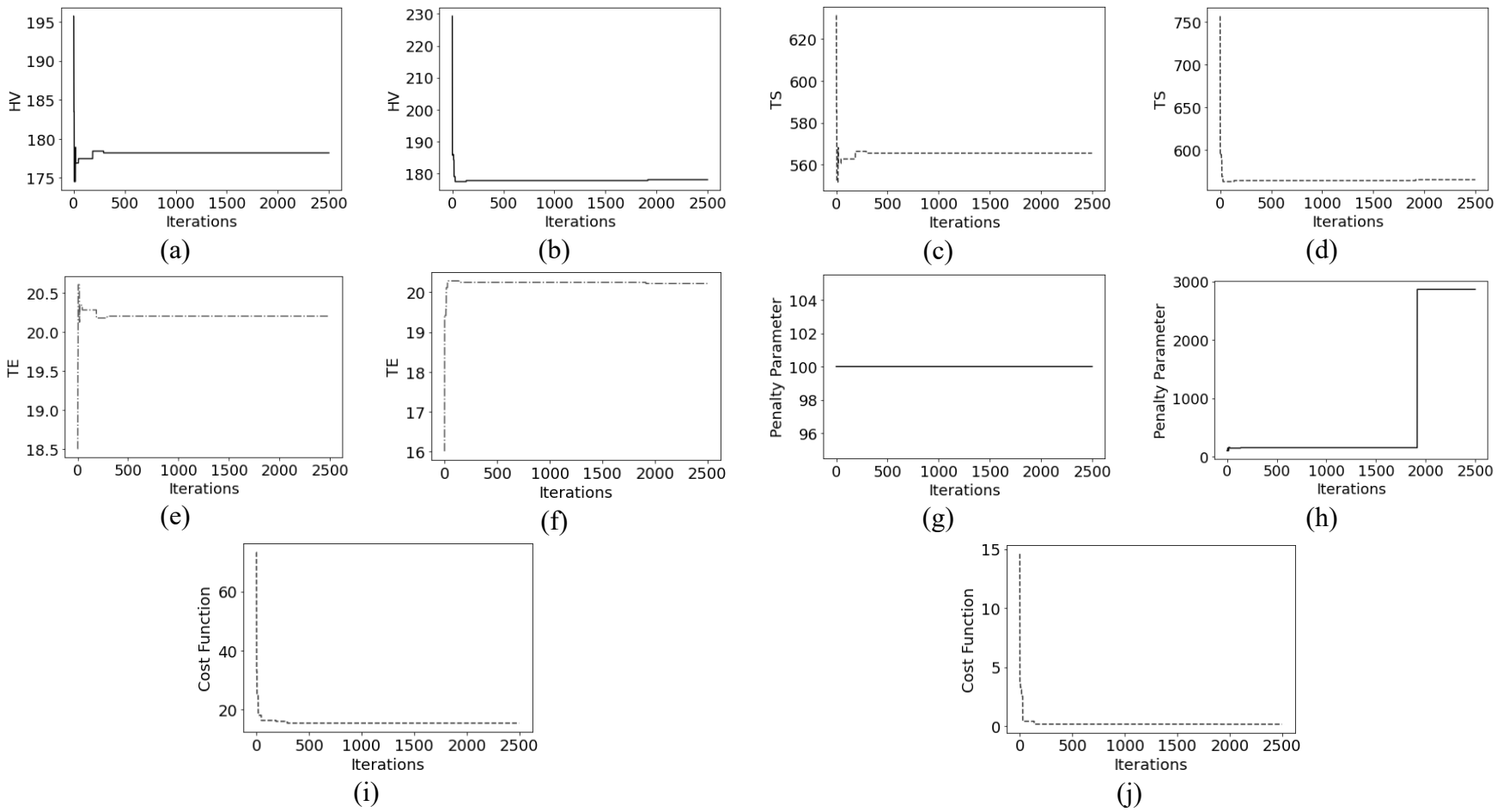

Figure 4-4: Results of the μGA for Cases H1 and H2 for AISI 8620. (a - f) The Mechanical Properties – Hardness, Tensile Strength, and Elongation, (g, h) the Penalty parameters, (i, j) the Cost Functions, for the Two Cases Respectively Over 2500 Generations

For cases S1 and S2, emphasis was placed on the tensile strength, TS, where the weight S was increased by a factor of 10 for S1, and the exponents h and e, were increased by a factor of 10 for S2 while all other weights and exponents remained as 1. Regardless of the shift in emphasis, the algorithm produced steels that met the target HV and TS values with accuracies of 100%. However, the elongation's, TE, accuracy was lower at 71%. This is consistent with the results in the previous cases (baseline, H1 and H2). In both cases, a high chromium content steel was generated, with S1 producing a medium carbon content steel and S2 producing a low carbon content steel. Both these steels had predominantly ferrite-pearlite microstructures, like the baseline, H1 and H2 cases since they had similar chemical compositions and heat treatment conditions. However, some bainite microstructures were predicted in the case of S2 due to the rapid cooling it experienced. This rapid cooling also resulted in a cheaper steel, with a cost of $0.27 / 100g in comparison to S1 which experienced a much slower cooling process. The resulting mechanical properties, penalty parameters, and cost functions, over 2500 iterations are shown in Figure 4-5. The corresponding cooling profiles are shown in Figure 4-7 (c, d). Overall, the algorithm stabilized faster for case S1 compared to S2.

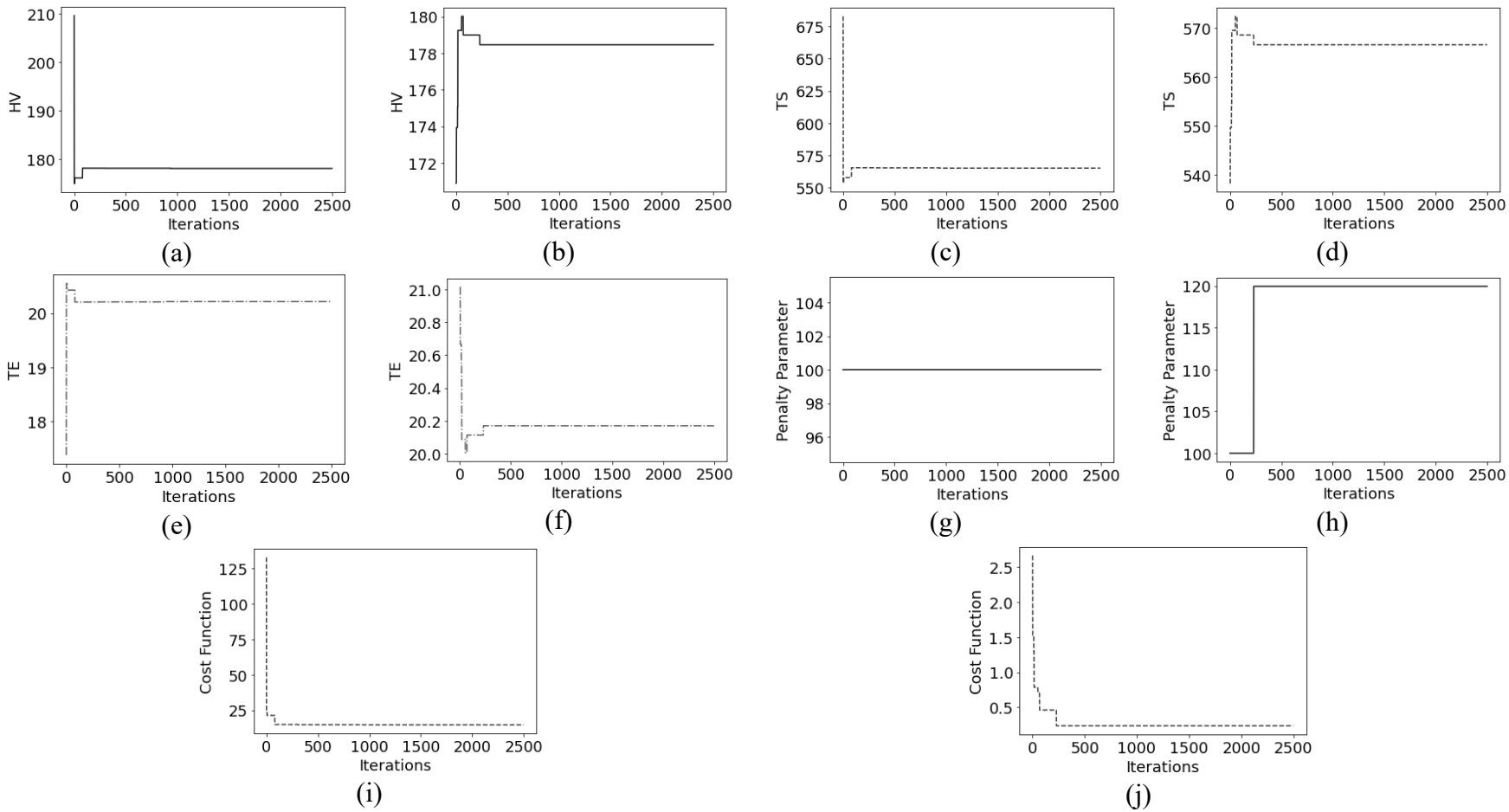

Figure 4-5: Results of the μGA for Cases S1 and S2 for AISI 8620. (a - f) The Mechanical Properties – Hardness, Tensile Strength, and Elongation, (g, h) the Penalty parameters, (i, j) the Cost Functions, for the Two Cases Respectively Over 2500 Generations

For an emphasis on elongation, TE, the weight E or the exponents h and s were increased by a factor of 10 for cases E1 and E2 respectively. Focussing on the elongation resulted in accuracies of 70%, 65% and 100% for HV, TS, and TE respectively. Overall, lower accuracies were calculated for hardness and tensile strength due to the correlation equation that was used. Although lower accuracies were received in these cases, highlighting the limitations of the TS-TE correlation equation, the predicted microstructure were consistent as is expected of a low carbon content steel with heat treatment conditions like for the cases S1 and S2. Like for S2, E1 exhibited a small percentage of bainite microstructure with the predominant structures being ferrite-pearlite due to its rapid cooling. E2 on the other hand had predominately ferrite-pearlite microstructures like S1 due to its slower cooling rate. Since E1 had lower chromium than in case S1, the ferrite microstructure was more dominant. Both these cases produced results that were cheaper than the baseline. This was due to the faster cooling profile for E1 and lower chromium content. For E2, it was mainly due to the lower chromium and Manganese contents as the cooling time was slightly longer for E2 in comparison to the baseline. These results are illustrated in Figure 4-6 for the mechanical property, penalty parameters and cost functions, and Figure 4-7 (e, f) for the cooling profile.

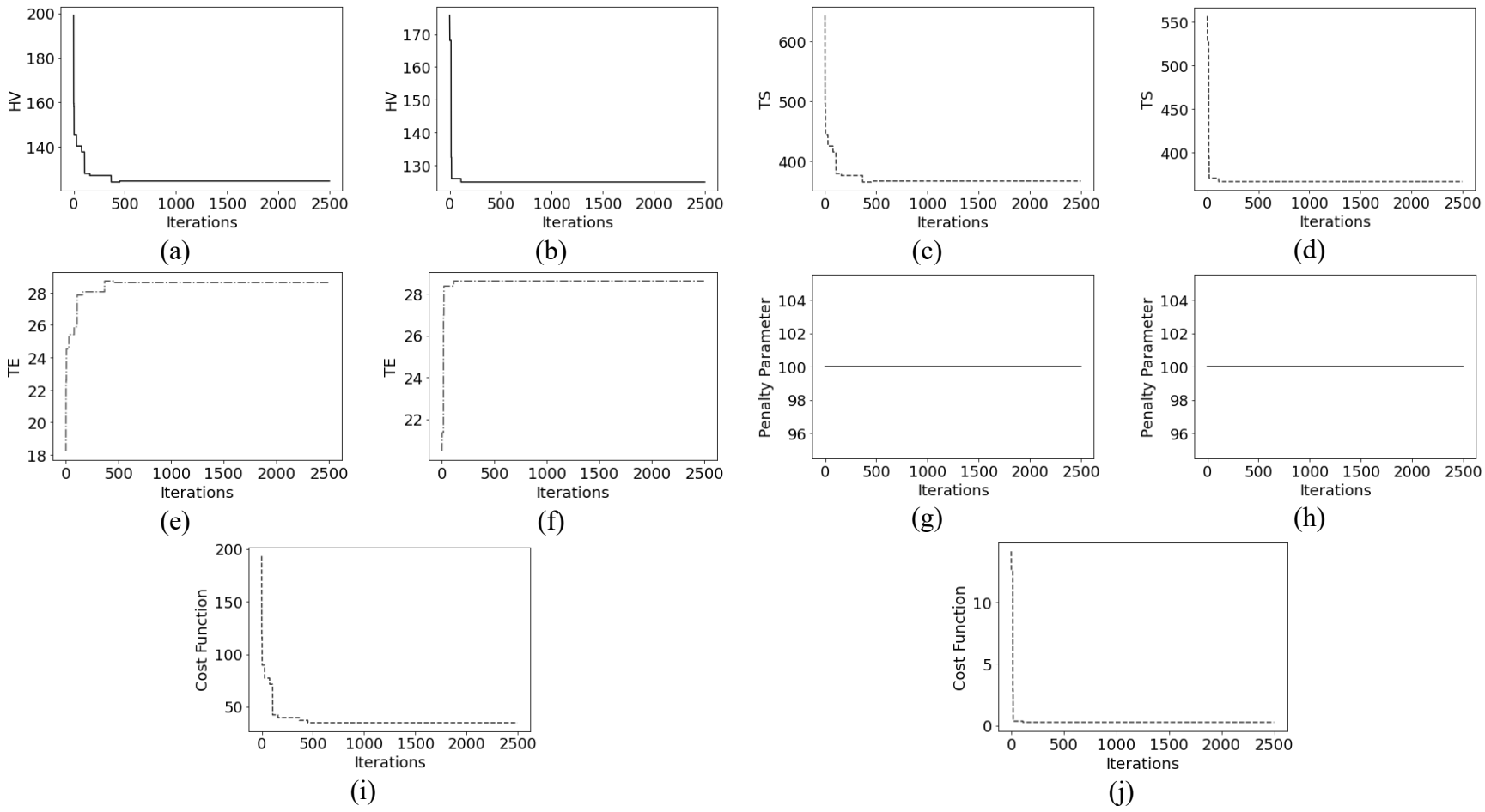

Figure 4-6: Results of the μGA for Cases E1 and E2 for AISI 8620. (a - f) The Mechanical Properties – Hardness, Tensile Strength, and Elongation, (g, h) the Penalty parameters, (i, j) the Cost Functions, for the Two Cases Respectively Over 2500 Generations

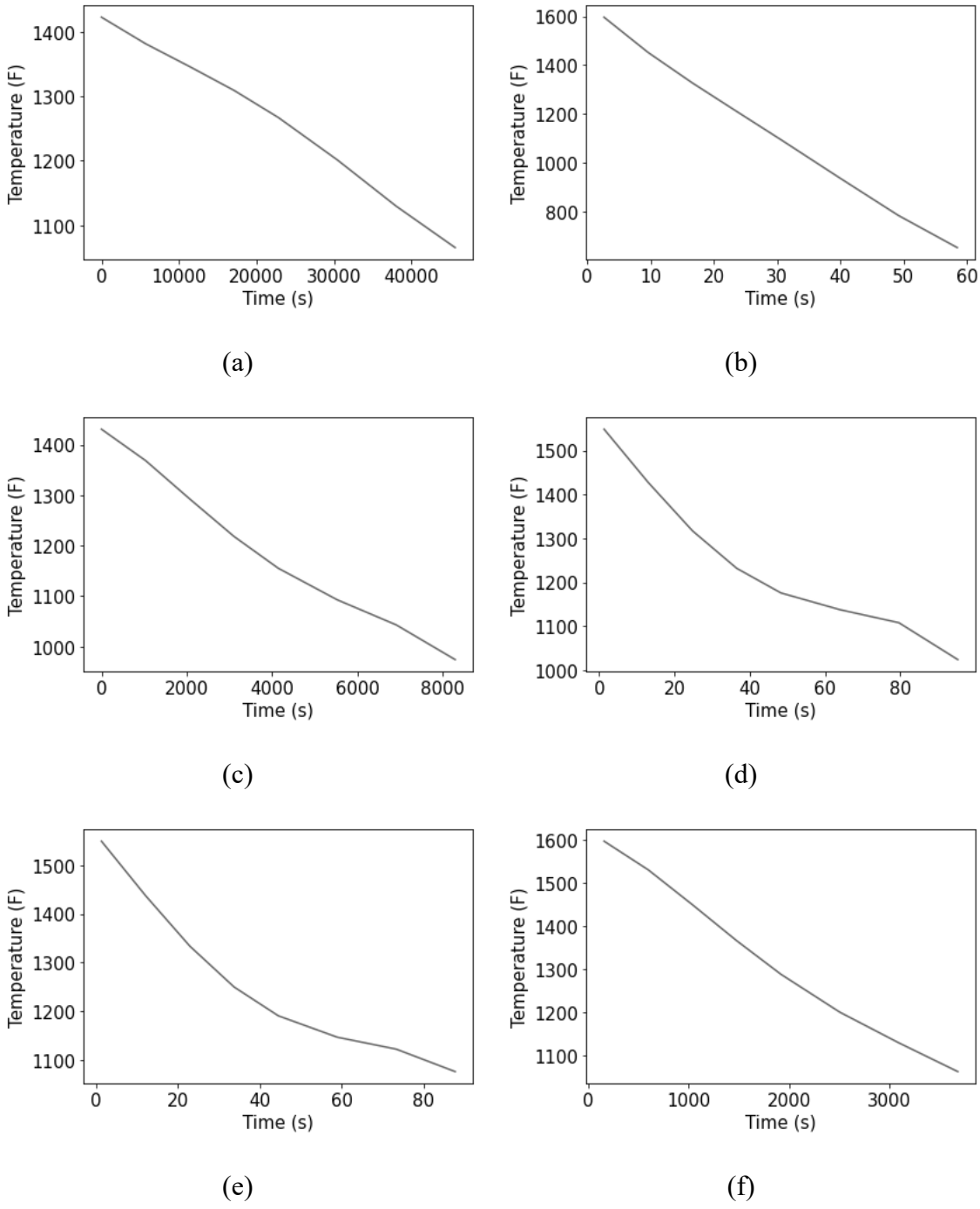

Figure 4-7: Resulting Cooling Profiles from the μGA for Cases H1, H2, S1, S2, E1 and E2 Respectively for AISI 8620

4.2.2 Optimization Results for Medium Strength Steels

The results based on the cases outlined in Section 3.5 are shown in Table 4-5 with their corresponding microstructure predictions in Table 4-6 for generated steels with AISI 4130 mechanical property targets.

Table 4-5: Algorithm Results for AISI 4130 for the Different Computational Cases

Cases	**Baseline**	**H1**	**H2**	**S1**	**S2**	**E1**	**E2**
Key parameters							
T_{aus} (F)	1807	1713	1816	1799	1670	1719	1555
CRave (F/s)	1719	1692	182	2	1717	46	14
C (wt. %)	0.44	0.27	0.25	0.19	0.47	0.54	0.32
Mn (wt. %)	0.65	0.98	0.70	0.97	0.89	0.63	0.22
P (wt. %)	0.03	0.01	0.01	0.01	0.01	0.00	0.01
S (wt. %)	0.02	0.02	0.01	0.01	0.00	0.01	0.02
Si (wt. %)	0.15	0.14	0.20	0.26	0.16	0.24	0.17
Ni (wt. %)	0.23	0.31	0.36	0.11	0.27	0.16	0.21
Cr (wt. %)	1.41	0.41	1.17	0.13	0.72	1.29	0.44
Mo (wt. %)	0.02	0.02	0.03	0.02	0.03	0.01	0.00
Cu (wt. %)	0.25	0.03	0.22	0.06	0.24	0.20	0.16
Al (wt. %)	0.01	0.00	0.00	0.00	0.00	0.00	0.00
V (wt. %)	0.00	0.01	0.01	0.00	0.01	0.00	0.00
B (wt. %)	0.00	0.00	0.00	0.00	0.00	0.00	0.00
N (wt. %)	0.00	0.00	0.00	0.00	0.00	0.00	0.00

Cases	Baseline	H1	H2	S1	S2	E1	E2
Ti (wt. %)	0.00	0.01	0.01	0.00	0.00	0.01	0.00
W (wt. %)	0.04	0.03	0.02	0.06	0.03	0.06	0.02
Mechanical Properties and Cost							
HV	272.3	286.0	286.1	272.6	272.3	190.2	190.1
TS (MPa)	916.9	968.1	968.4	918.1	916.9	610.4	610.1
TE (%)	13.7	13.1	13.1	13.7	13.7	19.0	19.0
Optimal Cost ($/100g)	0.34	0.25	0.32	0.33	0.24	0.30	0.17

Table 4-6: Microstructure Predictions for AISI 4130 for the Different Cases

Cases	Microstructure (%)					
	Austenite	Ferrite	Pearlite	Bainite	Martensite	Error
Baseline	0	3	95	2	0	0
H1	0	49	35	11	1	4
H2	0	17	41	37	5	0
S1	0	19	77	3	0	1
S2	0	12	75	13	0	0
E1	0	3	92	5	0	0
E2	0	40	55	2	0	3

For the baseline case, the weights and exponents in the cost objective function were equal to 1. In this case, a low alloy steel with a medium carbon content was generated from the algorithm producing accuracies of 95%, 100% and 72% for HV, TS, and TE respectively. Figure 4-8 (a – c) show the change of these properties over 2500 iterations. Figure 4-8 (d) shows the generated cooling profile. The values stabilize at around 250 iterations allowing for a more exhaustive search within the space for the remainder of the iterations. The cost function shows a similar trajectory to the mechanical property predictions as shown in Figure 4-8 (f). The penalty parameter in this case remained unchanged as a high starting penalty was chosen. This is shown in Figure 4-8 (e). The microstructure for the generated population was predicted to predominately consist of ferrite and pearlite as expected. This is supported with the expected results documented in the ASM Handbook [37].

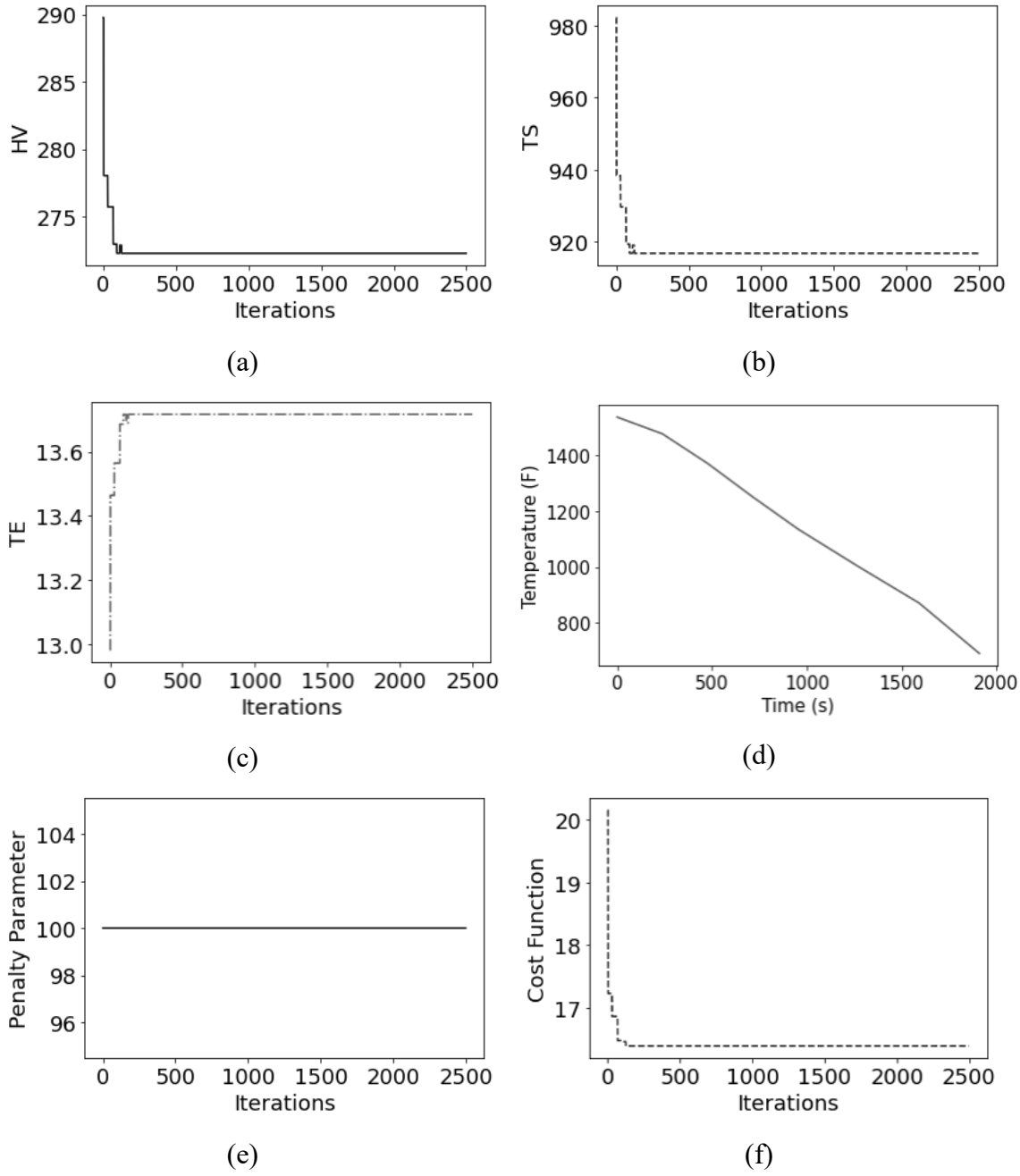

Figure 4-8: Results of the μGA for the Baseline Case for AISI 4130. (a – c) The Mechanical Properties – Hardness, Tensile Strength, Elongation, (d) the Cooling profile, (e) the Penalty Parameter, and (f) the Cost Function

To emphasize hardness, the weight H or the exponents s and e, were raised to the value of 10. In the case of H1, H was raised to 10 leaving the remaining weights and exponents equal to 1. In the case of H2, s and e, were raised to 10 leaving the remaining weights and exponents at 1. Both these cases produced similar results in terms of accuracy with values being 100%, 94% and 69% for HV, TS, and TE respectively. Figure 4-9 (a – f) shows these mechanical properties. Unlike the baseline case, it took around 1250 iterations in H1 and around 1500 iterations in H2, for the mechanical property predictions to stabilize. Moreover, both these cases produced low alloy steels with a medium carbon content. Overall, the contents were similar, only differing in manganese and chromium contents. For H1, the higher manganese decreased brittleness and therefore increased strength [38]. For H2, the increase in hardness and therefore strength was accomplished with the higher chromium [36]. Although the cooling profiles, shown in Figure 4-12 (a, b), of both these cases significantly vary in duration, with H2 heat treatment conditions lasting significantly longer, both cases generally produced similar microstructures. This is because their chemical composition was generally the same. As expected, the microstructure also predominately contained ferrite and pearlite as outlined in the ASM handbook [37] since it is a low alloy steel. Bainite was also present due to the combination of increased cooling rates and the presence of higher manganese or chromium. The optimal cost decreased from the baseline for case H1 due to the lower chromium content and is similar for H2 which has a similar chromium content to the baseline. The change of the penalty parameters for each case are shown in Figure 4-9 (g, h) and the cost functions are shown in Figure 4-9 (i, j).

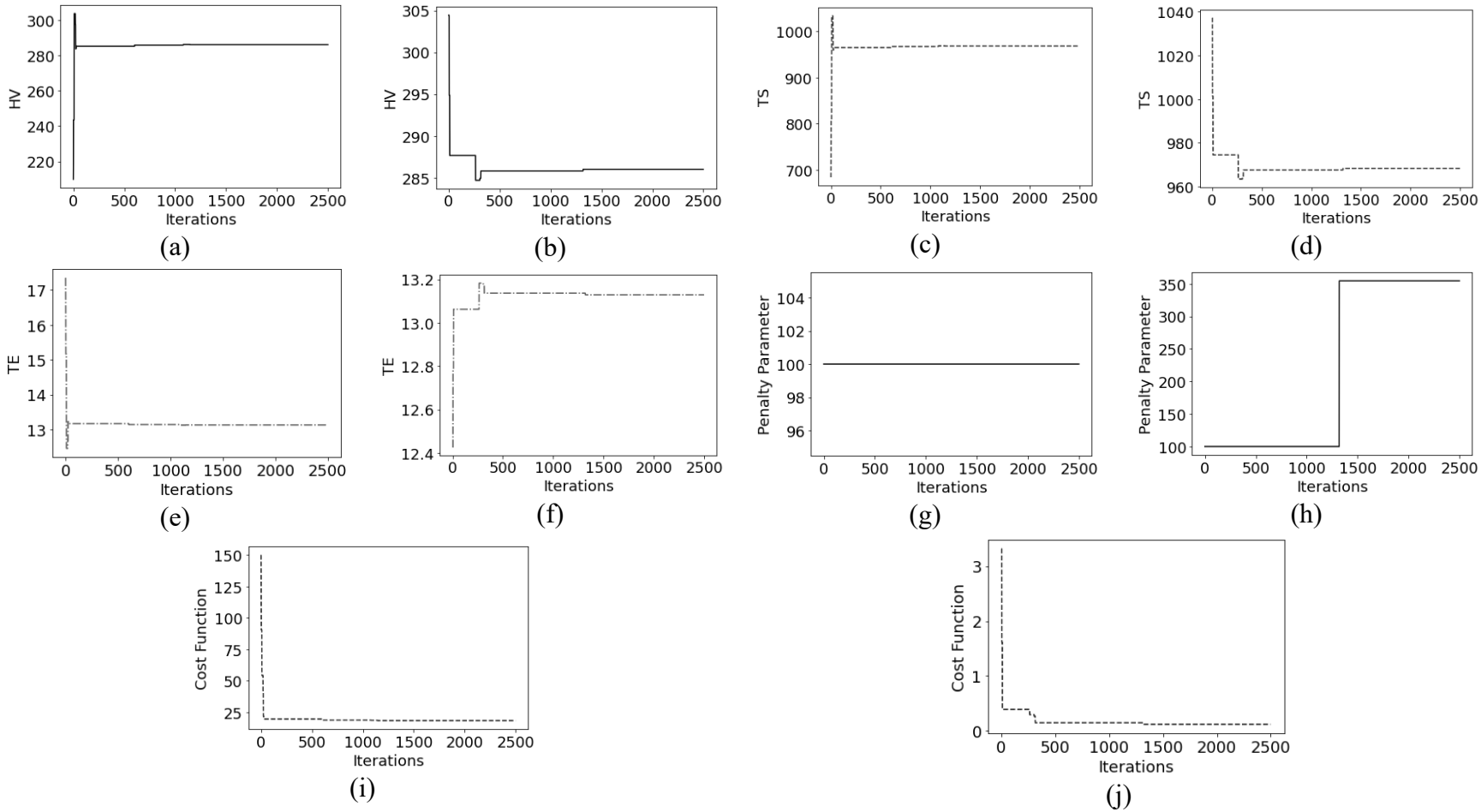

Figure 4-9: Results of the μGA for Cases H1 and H2 for AISI 4130. (a - f) The Mechanical Properties – Hardness, Tensile Strength, and Elongation, (g, h) the Penalty parameters, (i, j) the Cost Functions, for the Two Cases Respectively Over 2500 Generations

In both S1 and S2 cases, the focus was shifted to the mechanical property TS, leading to an increased accuracy in this area. As such, the runs yielded accuracies of 95%, 100% and 72% for HV, TS, and TE respectively in both cases. With the increased emphasis on TS however, a slightly lower accuracy for the HV property was produced compared to the previous case. Nevertheless, the results remained consistent with those of the baseline case. However, unlike this baseline, case S1 stabilized after 1250 iterations, while S2 required 1500 iterations. Moreover, the μGA produced a low alloy steel with a low carbon content for S1 and a medium carbon content for S2. S2 had higher levels of chromium, nickel, and copper which improved hardenability and overall mechanical properties [36]. S1 had a lower average cooling rate than S2 as shown in Table 4-5 resulting in longer TMP times and a predominately ferrite-pearlite microstructure. Conversely, S2 had a higher average cooling rate resulting in an increased amount of bainite in its microstructure. The predicted microstructure for these cases is shown in Table 4-6, and the cooling profiles in Figure 4-12 (c, d). The change of the penalty parameters for each case is shown in Figure 4-10 (g, h). There was a step change in penalty parameters for case S2 while case S1 remained constant. The corresponding cost functions are shown in Figure 4-10 (i, j).

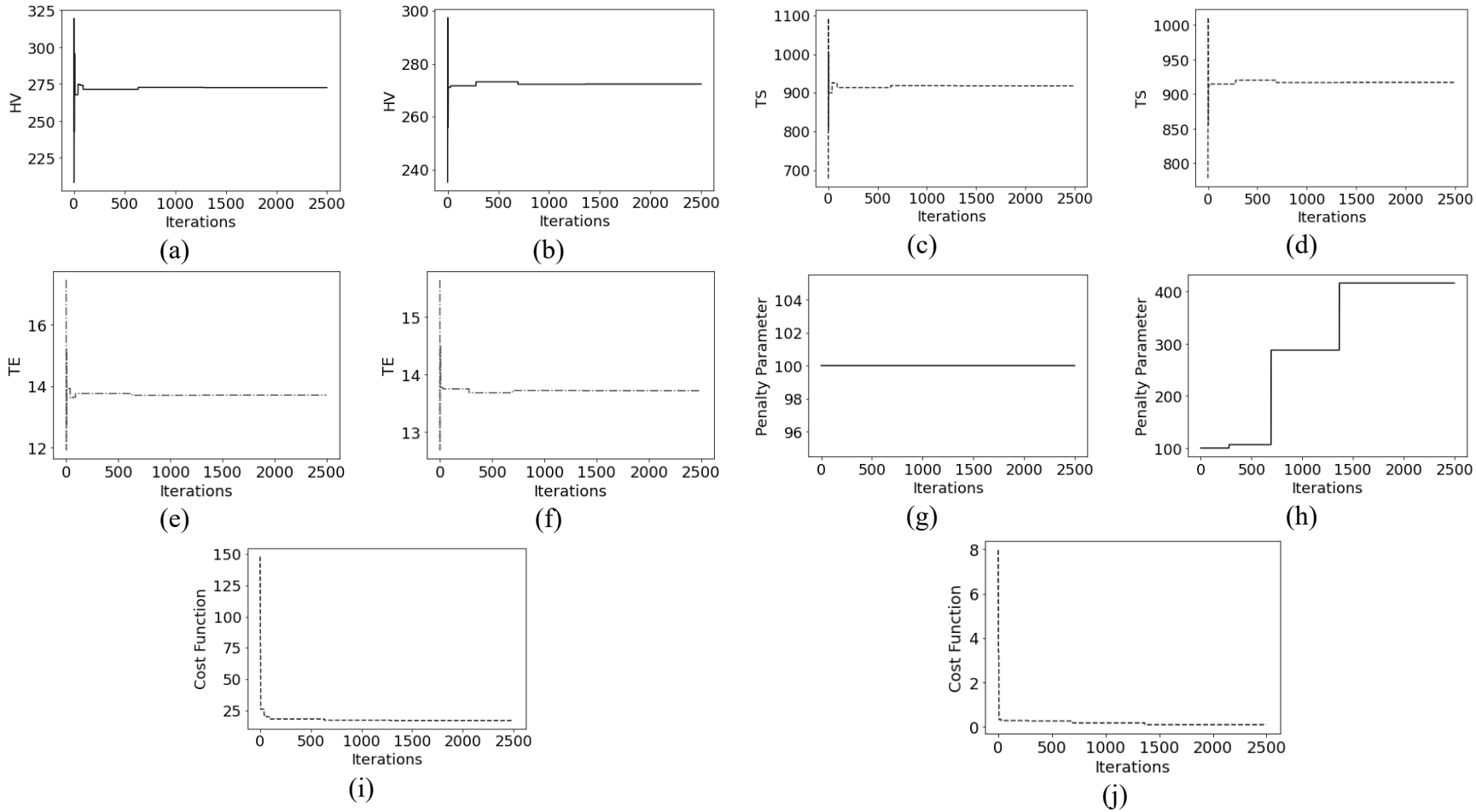

Figure 4-10: Results of the μGA for Cases S1 and S2 for AISI 4130. (a - f) The Mechanical Properties – Hardness, Tensile Strength, and Elongation, (g, h) the Penalty parameters, (i, j) the Cost Functions, for the Two Cases Respectively Over 2500 Generations

Finally, to emphasize TE, either the weight E or the exponents h and s could be increased. In E1, only the weight E was increased, whereas in E2, the exponents h and s were increased. Both cases yielded comparable results, with E2 having a slightly lower accuracy for HV. More precisely, the results were 67%, 67%, and 100% for HV, TS, and TE, respectively in case E1, and 66%, 67%, and 100% for HV, TS, and TE, respectively in case E2. Figure 4-11 (a – f) shows the evolution of these properties over 2500 iterations, where optimal solution was achieved at around 125 iterations. Although it took fewer iterations to find an optimal solution compared to the other cases, the HV and TS accuracies were very low due to the correlation equation used. Ultimately, meeting the target elongation was at the expense of HV and TS. For these cases, a low alloy steel with a high carbon content was generated for E1 and a medium carbon steel was obtained for E2. E1 had a higher Cr content, thus increasing hardenability and resulting in a slightly higher HV. However, neither case had the appropriate composition to meet HV and TS targets, reflecting in the poor accuracy values for these properties. Additionally, E2 had a slower cooling rate than E1 as shown in Table 4-5 and Figure 4-12 (e, f) indicating a slightly longer TMP time. This processing time, in combination with the predicted HV results, led to a predominately ferrite-pearlite microstructure. The penalty parameters for both cases are shown in Figure 4-11 (g, h). Like the previous two cases, the penalty parameter for case E2 changed with the iterations before stabilizing, while the penalty parameter for case E1 remained constant. The corresponding cost functions for the cases are shown in Figure 4-11 (i, j).

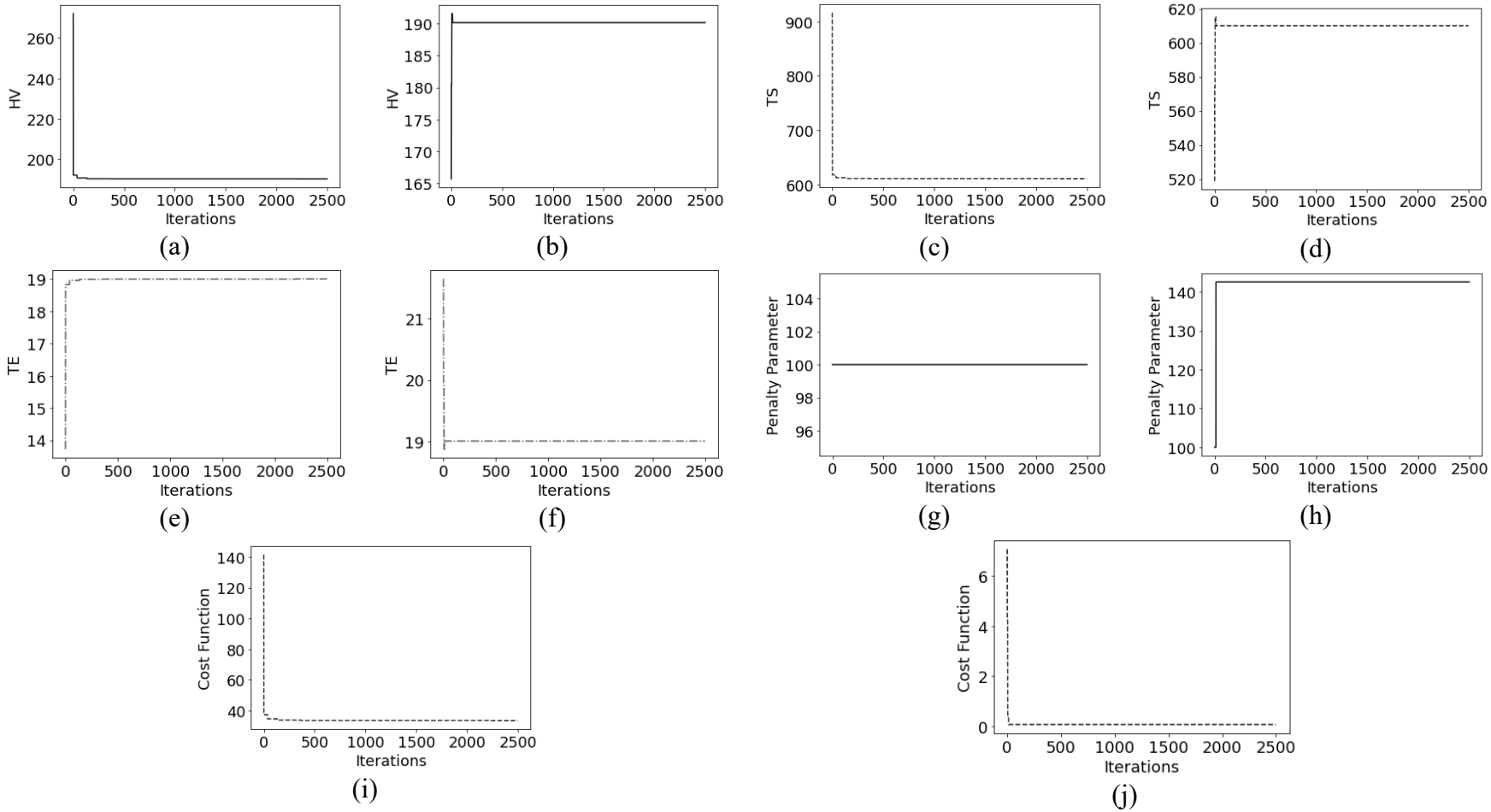

Figure 4-11: Results of the μGA for Cases E1 and E2 for AISI 4130. (a - f) The Mechanical Properties – Hardness, Tensile Strength, and Elongation, (g, h) the Penalty parameters, (i, j) the Cost Functions, for the Two Cases Respectively Over 2500 Generations

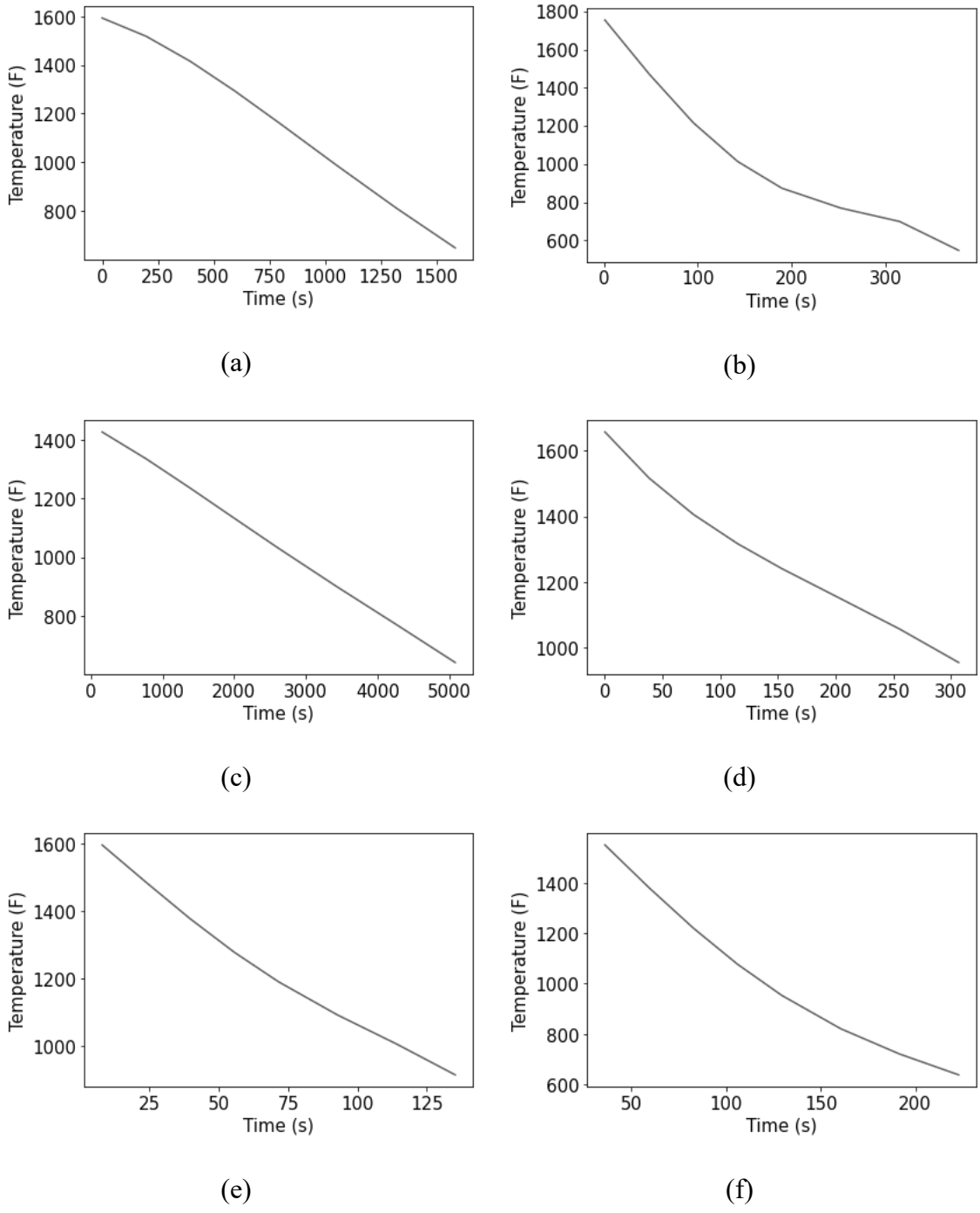

Figure 4-12: Resulting Cooling Profiles from the μGA for Cases H1, H2, S1, S2, E1 and E2 Respectively for AISI 4130

4.2.3 Optimization Results for High Strength Steels

Table 4-7 shows the algorithm results for generated steels with 420 Stainless Steel mechanical property targets. Table 4-4 shows the corresponding microstructure predictions.

Table 4-7: Algorithm Results for 420 Stainless Steel for the Different Computational Cases

Cases	**Baseline**	**H1**	**H2**	**S1**	**S2**	**E1**	**E2**
Key parameters							
T_{aus} (F)	1695	1549	1737	1743	1531	1715	1578
CRave (F/s)	1894	2382	197	196	399	301	18
C (wt. %)	0.13	0.21	0.27	0.13	0.49	0.51	0.22
Mn (wt. %)	0.88	1.22	0.78	0.77	0.98	1.23	1.19
P (wt. %)	0.02	0.00	0.00	0.00	0.01	0.00	0.03
S (wt. %)	0.02	0.01	0.01	0.01	0.01	0.01	0.02
Si (wt. %)	0.34	0.17	0.20	0.24	0.32	0.16	0.38
Ni (wt. %)	0.30	0.18	0.03	0.11	0.03	0.03	0.04
Cr (wt. %)	0.93	1.35	0.21	1.19	0.71	0.39	1.08
Mo (wt. %)	0.02	0.01	0.03	0.03	0.02	0.01	0.02
Cu (wt. %)	0.09	0.15	0.16	0.15	0.20	0.26	0.13
Al (wt. %)	0.00	0.00	0.00	0.00	0.00	0.00	0.00
V (wt. %)	0.01	0.02	0.01	0.01	0.00	0.01	0.00
B (wt. %)	0.00	0.00	0.00	0.00	0.00	0.00	0.00
N (wt. %)	0.00	0.00	0.00	0.00	0.00	0.00	0.00

Cases	Baseline	H1	H2	S1	S2	E1	E2
Ti (wt. %)	0.00	0.00	0.00	0.01	0.01	0.00	0.00
W (wt. %)	0.06	0.07	0.03	0.04	0.06	0.01	0.07
Mechanical Properties and Cost							
HV	483.4	525.0	525.0	483.4	483.4	277.2	277.4
TS (MPa)	1705.4	1860.7	1860.4	1705.4	1705.4	935.1	935.8
TE (%)	8.3	7.8	7.8	8.3	8.3	13.5	13.5
Optimal Cost ($/100g)	0.35	0.32	0.18	0.30	0.28	0.19	0.36

Table 4-8: Microstructure Predictions for 420 Stainless Steel for the Different Cases

Cases	Microstructure (%)					
	Austenite	Ferrite	Pearlite	Bainite	Martensite	Error
Baseline	0	0	0	6	94	0
H1	0	0	0	0	100	0
H2	0	0	0	0	100	0
S1	0	0	0	0	100	0
S2	0	0	0	0	100	0
E1	0	0	0	24	76	0
E2	0	0	0	33	66	1

In the baseline case where all the weights and exponents were set to 1, the algorithm successfully generated a medium carbon content steel with high manganese and chromium contents. These chemical compositions improved the steel's strength and consequently its hardness. Mechanical property prediction showed that the generated steel exhibited high accuracy for hardness (HV) and tensile strength (TS) properties, with results of 92% and 100% respectively. However, there is room for improvement for the elongation property, which, showed a lower accuracy at 62%, largely due to the tensile strength, elongation, correlation equation used. These results are illustrated in Figure 4-13. Although it took 750 for the results to stabilize, there were still enough iterations left to explore the search space more exhaustively with the remaining 1750 iterations.

In this case, the steel was rapidly cooled for about two and half minutes resulting in a predominantly martensitic microstructure as shown in Table 4-8 and as expected according to previous literature [11], [13], [32]. This rapid cooling and generally mid-range chemical compositions with higher chromium content contributed to the steel's overall cost of $0.35 / 100g.

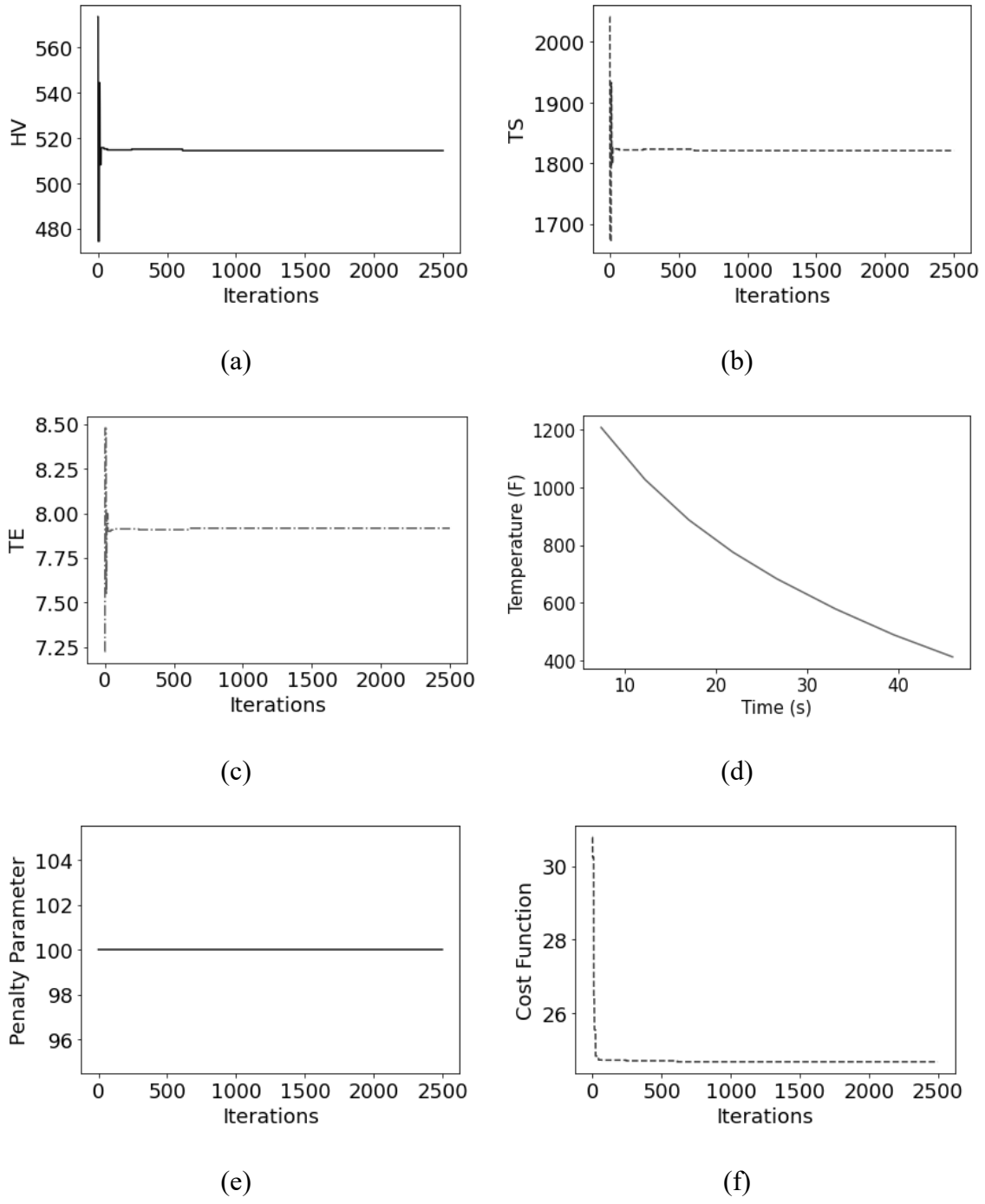

Figure 4-13: Results of the μGA for the Baseline Case for 420 Stainless Steel. (a – c) The Mechanical Properties – Hardness, Tensile Strength, Elongation, (d) the Cooling profile, (e) the Penalty Parameter, and (f) the Cost Function

For cases H1 and H2, the algorithm optimized for the hardness mechanical property. This optimization was achieved by either increasing H by a factor of 10 or the coefficients s and e, by a factor of 10 while keeping the other weights and coefficients as 1. In both cases, a medium carbon content steel was generated with H2 having a significantly higher chromium content and slightly higher manganese content than H1. These alloys increased the steels hardness allowing for the target to be met.

Overall, the algorithm produced accurate results for HV and TS with 100% and 91% accuracies respectively. Lower accuracies were produced for TE with 58% accuracy. The lower accuracy in TS was attributed to the correlation equation used between HV and TS as this diverged at higher tensile strength targets. Similarly, lower accuracies for TE was also be attributed to the correlation equation used between TS and TE. Regardless of these results, the cost per 100 g of the generated steels was less than the baseline. This was mainly attributed to the rapid cooling that was generated. Due to this heat treatment profile as shown in Figure 4-17, a martensitic microstructure was expected and was predicted by the microstructure prediction model. The microstructure was predicted to be 100% martensitic in both cases. This prediction is shown in Table 4-8, and the mechanical property, penalty parameters, and cost functions outcomes, for 2500 iterations are shown in Figure 4-14.

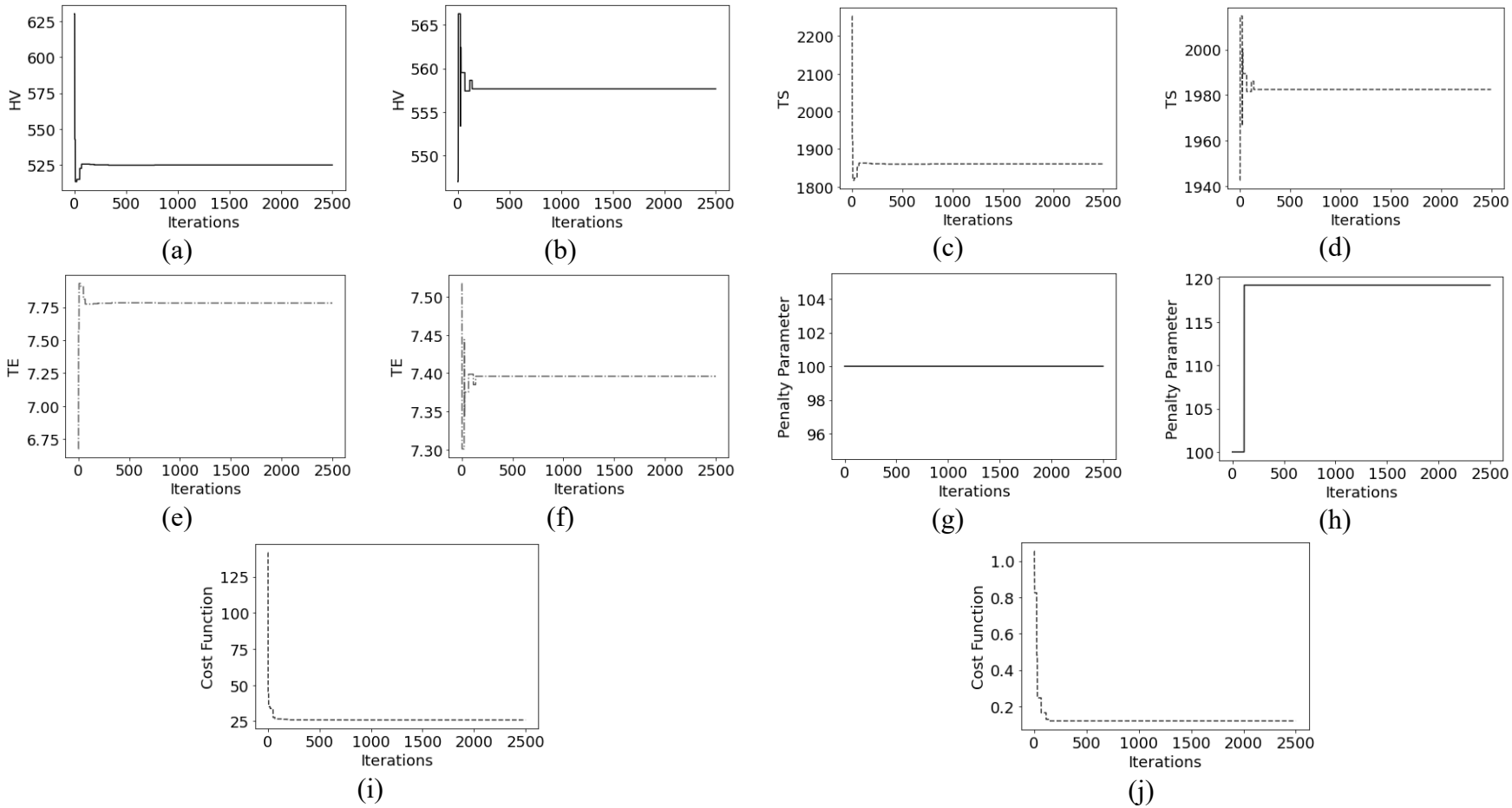

Figure 4-14: Results of the μGA for Cases H1 and H2 for 420 Stainless Steel. (a - f) The Mechanical Properties – Hardness, Tensile Strength, and Elongation, (g, h) the Penalty parameters, (i, j) the Cost Functions, for the Two Cases Respectively Over 2500 Generations

In the case of S1 and S2, the weight S or the exponents h and e, were raised by a factor of 10 respectively, leaving the remainder of the constants as 1 with the objective of optimizing for tensile strength. The populations generated met the target with 92%, 100%, and 62% accuracy for HV, TS, and TE respectively. For S1, the cost was comparable to all previous cases for this target especially the baseline. However, the results for this case had a lower carbon content, and shorter heat treatment time. As such, the microstructure present was also martensitic, with some percentage of bainite being predicted. Similar results were seen for case S2 with comparable cost to cases S1 and H1. For this generation a rapidly cooled medium carbon content steel with similar levels of manganese and chromium to the baseline was generated. Due to this rapid cooling a presence of martensite was expected, and it was confirmed with the microstructure prediction shown in Table 4-8. The corresponding cooling profiles are shown in Figure 4-17. The mechanical property outcomes, penalty parameters and cost functions for the 2500 iterations are shown in Figure 4-15.

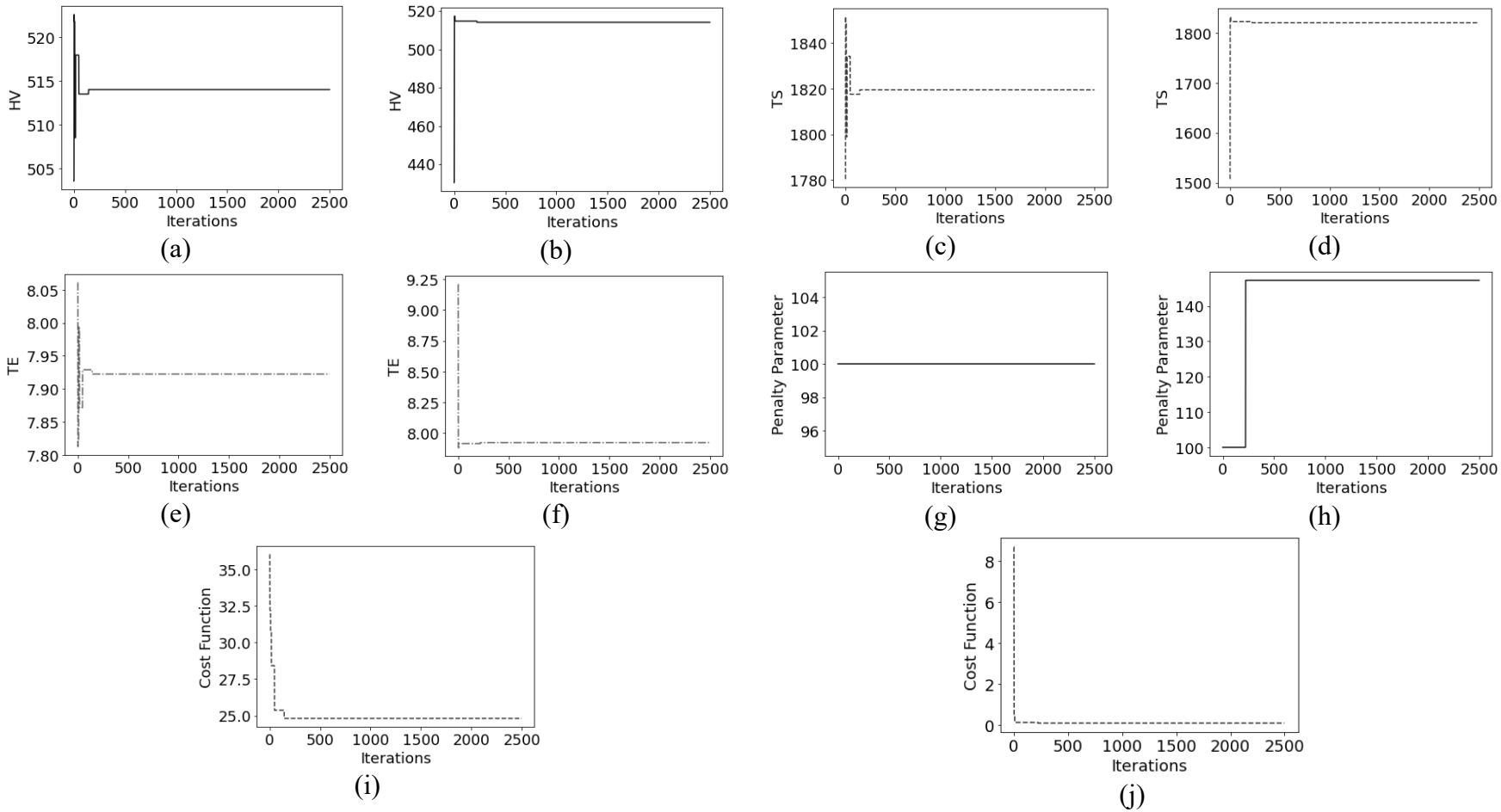

Figure 4-15: Results of the μGA for Cases S1 and S2 for 420 Stainless Steel. (a - f) The Mechanical Properties – Hardness, Tensile Strength, and Elongation, (g, h) the Penalty parameters, (i, j) the Cost Functions, for the Two Cases Respectively Over 2500 Generations

For E1 and E2, the weights and exponents were modified with the objective of optimizing for the material's elongation. The weight E was increased by a factor of 10 in the case of E1 and the exponents h and s were increased by a factor of 10 in the case of E2. The remainder of the weights and exponents were left as 1. Through this, the generated populations met the target for elongation at the detriment of the other two properties due to the correlation equations used. Results were 53%, and 55% for HV and TS respectively to achieve 100% accuracy for TE. Since the hardness and tensile properties were underestimated, the overall cost for E1 was amongst the cheapest for the specified targets. The cost for E2 was more comparable to the baseline due to the slower cooling and higher chromium content. This higher chromium content and relatively fast heat treatment times, coupled with the low predicted hardness produced steels with a large percentage of martensite within the microstructure, with a small percentage of bainite also present. Figure 4-16 shows the predicted material properties, penalty parameters and cost functions over 2500 iterations. The corresponding microstructure predictions are shown in Table 4-8 and their cooling profiles in Figure 4-17.

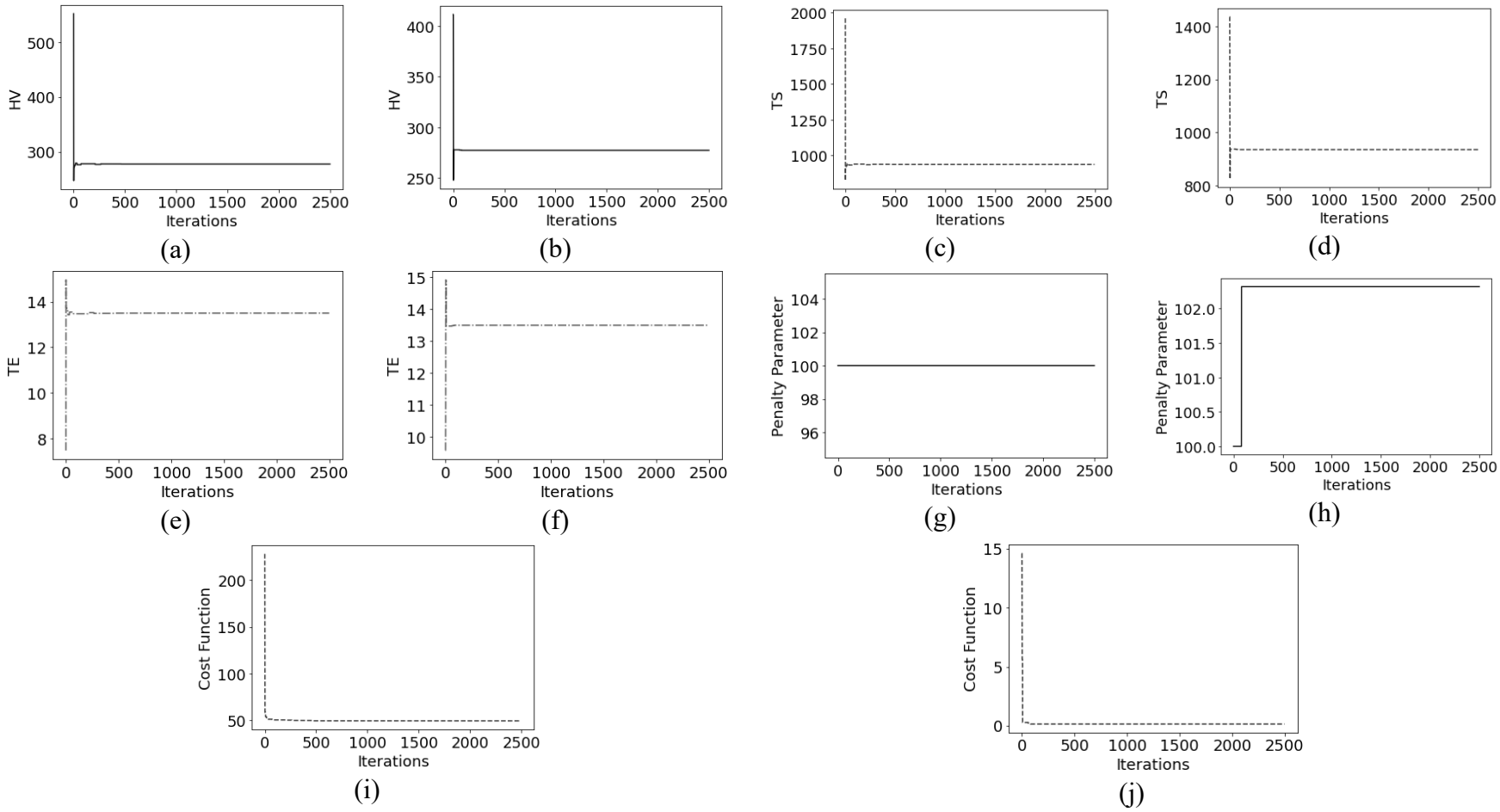

Figure 4-16: Results of the μGA for Cases E1 and E2 for 420 Stainless Steel. (a - f) The Mechanical Properties – Hardness, Tensile Strength, and Elongation, (g, h) the Penalty parameters, (i, j) the Cost Functions, for the Two Cases Respectively Over 2500 Generations

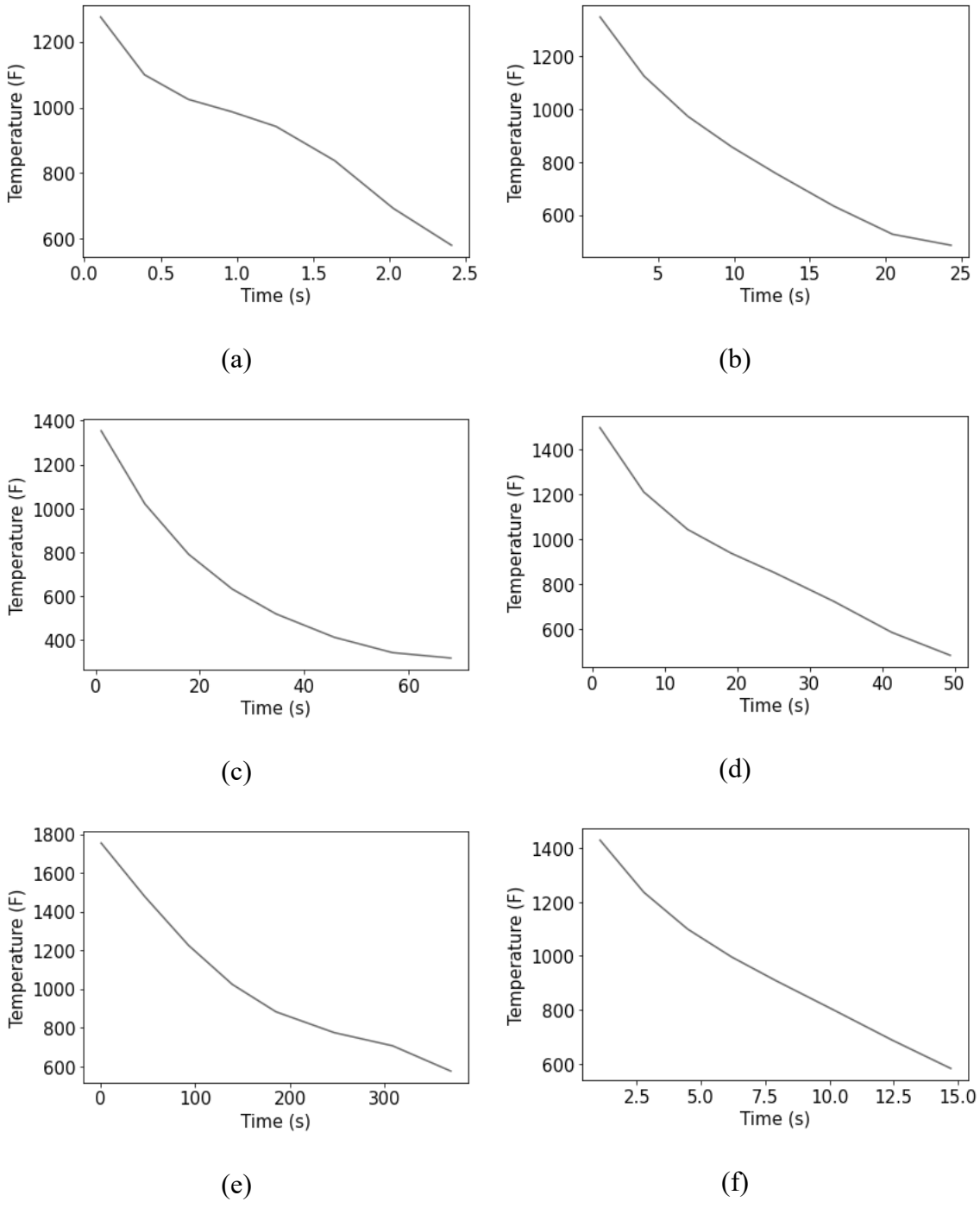

Figure 4-17: Resulting Cooling Profiles from the μGA for Cases H1, H2, S1, S2, E1 and E2 Respectively for 420 Stainless Steel

4.3 Optimizing for Cost Results

To assess whether the algorithm could generate more cost-effective results than a standard steel with chemical compositions and TMP retrieved from the ATLAS [28], three different runs were performed for each specific target. The theoretical costs selected from the ATLAS [28] were calculated. For the algorithm to be successful, a cost lower than the theoretical costs must be generated. For these runs, HV was emphasized by increasing the exponent s and e by a factor of 10, since the results from the previous test cases consistently showed relatively low costs when those exponents were modified. To ensure that the cost was further minimized, the cost weight, C, was also changed to an arbitrary value of 10. The results of the three runs are shown in Table 4-9, Table 4-10, and Table 4-11 for the low, medium, and high strength steel respectively. Figure 4-18 shows the corresponding cooling profiles for all the target cases.

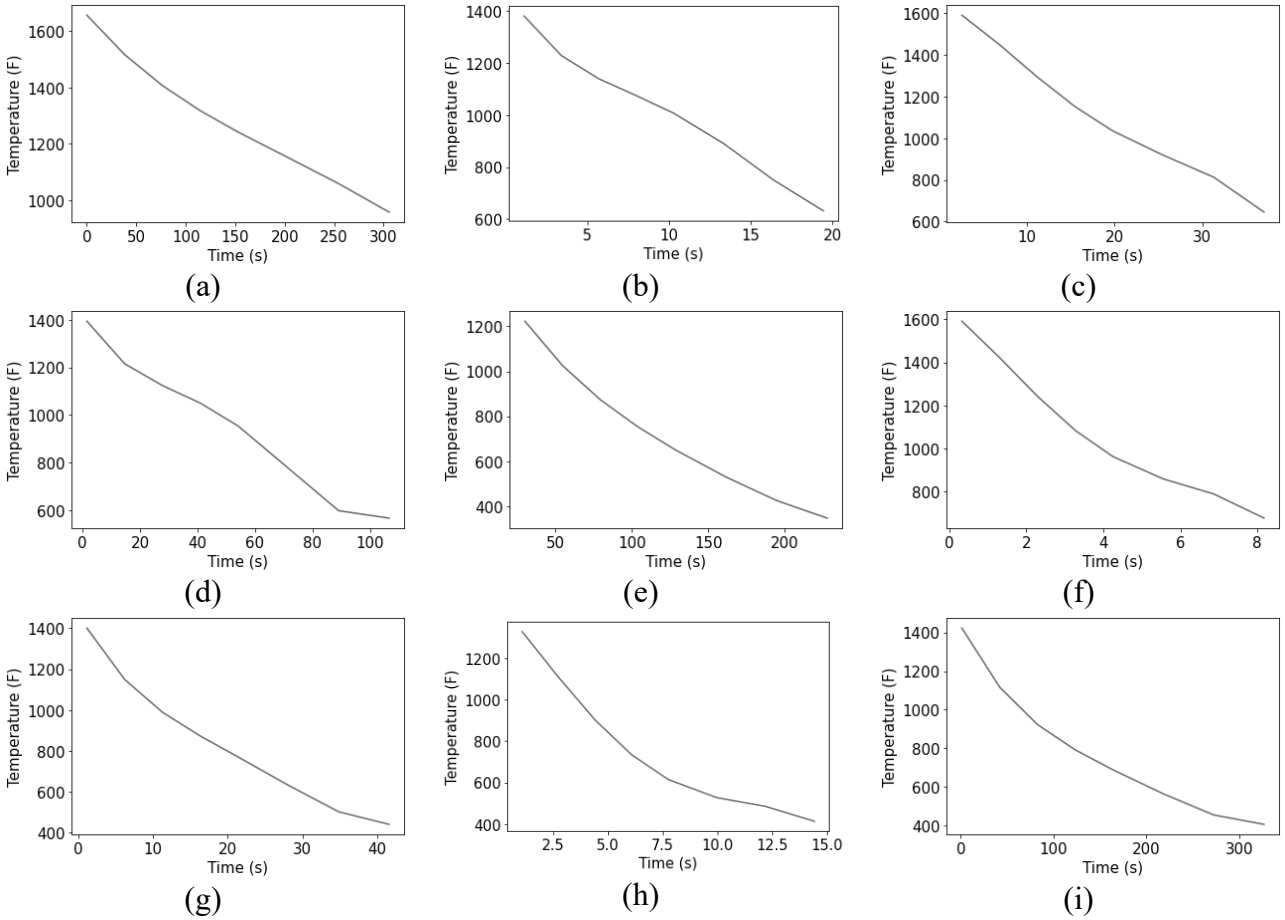

Figure 4-18: Cooling Profiles for the Optimization Test Cases. (a – c) Runs 1 – 3 for AISI 8620 Targets, (d – f) Runs 1 – 3 for AISI 4130 Targets, and (g – i) Runs 1- 3 for 420 Stainless Steel Targets, respectively.

For the AISI 8620 target, which is a low alloy low carbon content steel, the three runs generated low and medium carbon content steels. These generated steels had a predominantly pearlite-ferrite microstructure, as expected for a low strength steel with a mid-range carbon content. All runs achieved 100% accuracy for HV and were more cost effective than the theoretical alloy which cost \$0.31 / 100g resulting in savings of more than \$0.15 / 100g. Overall, runs 1 and 2 were the cheapest of the three making them the best option for the cost optimization; however, all three runs successfully applied the algorithm to optimize for the cost while still meeting the hardness and tensile strength target.

Table 4-9: Results of the μGA for the Optimal Cases with Cost Optimization (i.e., for C = 10, s = 10, e = 10) for AISI 8620 Target

	Theoretical	**Run 1**	**Run 2**	**Run 3**
Chemical Composition (wt. %)				
C	0.21	0.34	0.46	0.15
Mn	0.71	0.54	0.25	0.68
P	0.00	0.02	0.03	0.00
S	0.01	0.02	0.01	0.01
Si	0.30	0.15	0.18	0.18
Ni	0.63	0.35	0.04	0.13
Cr	0.49	0.09	0.00	0.34
Mo	0.17	0.02	0.02	0.02
Cu	0.01	0.10	0.25	0.16

	Theoretical	Run 1	Run 2	Run 3
Al	0.01	0.00	0.00	0.00
V	0.00	0.00	0.01	0.01
B	0.00	0.00	0.00	0.00
N	0.00	0.00	0.00	0.00
Ti	0.00	0.01	0.01	0.00
W	0.00	0.06	0.07	0.03
Mechanical Properties, Phase Composition, and Cost				
HV	178.0	178.1	178.5	178.0
Cost ($/100g)	0.31	0.15	0.15	0.18
Austenite	0	0	0	0
Ferrite	52	52	2	66
Pearlite	48	42	91	26
Bainite	0	2	6	3
Martensite	0	0	1	0
Microstructure Error	0	4	0	5

This success was further proved in the cost optimization for the AISI 4130 mechanical property targets. In contrast to the previous targets that produced low-medium carbon content steels, this trial generated results that spanned the entire low to high carbon content spectrum. Significantly, all runs had lower chromium contents than the theoretical steel, contributing to the cost savings. While some of the generated steels were close in cost

to the theoretical steel, they were all still cheaper to produce, with the third run being the most cost effective. In this run, the cost of producing a steel with 100% accuracy for the hardness mechanical property, was more than halved. In line with the theoretical steel, all the runs had a combination of a predominantly ferrite, pearlite, and bainite microstructure, with a small percentage of martensite.

Table 4-10: Results of the μGA for the Optimal Cases with Cost Optimization (i.e., for C = 10, s = 10, e = 10) for AISI 4130 Target

	Theoretical	**Run 1**	**Run 2**	**Run 3**
Chemical Composition (wt. %)				
C	0.30	0.47	0.19	0.53
Mn	0.64	0.72	0.90	0.63
P	0.01	0.03	0.03	0.03
S	0.01	0.02	0.01	0.00
Si	0.22	0.21	0.28	0.15
Ni	0.11	0.14	0.36	0.05
Cr	1.01	0.24	0.04	0.27
Mo	0.24	0.02	0.00	0.02
Cu	0.19	0.26	0.19	0.25
Al	0.00	0.00	0.00	0.00
V	0.01	0.01	0.01	0.00
B	0.00	0.00	0.00	0.00
N	0.00	0.00	0.00	0.00

	Theoretical	Run 1	Run 2	Run 3
Ti	0.00	0.00	0.01	0.00
W	0.00	0.00	0.04	0.01
Mechanical Properties, Phase Composition, and Cost				
HV	286.0	286.1	286.0	286.2
Cost ($/100g)	0.33	0.20	0.23	0.14
Austenite	0	0	0	0
Ferrite	10	6	12	4
Pearlite	0	45	7	75
Bainite	80	40	53	19
Martensite	10	9	28	2
Microstructure Error	-	-	-	-

In addition to the successful results for AISI 8620 and AISI 4130 mechanical property targets, similar runs were conducted for the 420 stainless steel mechanical property target case. In this case, all three runs generated a medium carbon content steel, like the theoretical steel. However, the generated steels had a significantly lower chromium content compensated for by higher manganese contents and faster heat processing times. Consequently, the overall cost of the generated steels was approximately seven times less expensive than the theoretical steel. Also, as expected, these steels had a martensitic microstructure. This demonstrated the effectiveness of the algorithm in the optimization of cost without comprising the mechanical property targets.

Table 4-11: Results of the μGA for the Optimal Cases with Cost Optimization (i.e., for C = 10, s = 10, e = 10) for 420 Stainless Steel Target

	Theoretical	**Run 1**	**Run 2**	**Run 3**
Chemical Composition (wt. %)				
C	0.44	0.49	0.20	0.34
Mn	0.20	1.04	0.89	0.76
P	0.03	0.03	0.03	0.02
S	0.01	0.01	0.01	0.00
Si	0.30	0.18	0.18	0.15
Ni	0.31	0.13	0.31	0.26
Cr	13.12	0.59	0.10	0.45
Mo	0.01	0.01	0.00	0.02
Cu	0.09	0.25	0.07	0.04
Al	0.00	0.00	0.00	0.00
V	0.02	0.00	0.00	0.01
B	0.00	0.00	0.00	0.00
N	0.00	0.00	0.00	0.00
Ti	0.00	0.00	0.01	0.00
W	0.00	0.02	0.01	0.07
Mechanical Properties, Phase Composition, and Cost				
HV	525.0	524.9	525.4	522.9
Cost ($/100g)	1.75	0.2	0.15	0.21

	Theoretical	Run 1	Run 2	Run 3
Austenite	0	0	0	0
Ferrite	0	0	0	0
Pearlite	5	0	0	0
Bainite	0	0	1	0
Martensite	95	100	99	100
Microstructure Error	-	-	-	-

Ultimately, the application of the developed algorithm demonstrated its effectiveness in optimizing for cost while preserving the desired mechanical properties, specifically hardness. The results from the AISI 8620, AISI 4130, 420 Stainless Steel runs, proved the versatility of the algorithm in producing steels of various alloying element contents to meet the different targets while reducing production cost to up to seven times.

4.4 Limitations and Future Work

The presented work has successfully developed an algorithm that optimizes for desired mechanical properties and cost. However, there are some limitations that must be considered. First, the accuracy of the algorithm decreases as the strength of the steel increases. As a result, it produces results with higher accuracies for lower strength steels compared to higher strength steels. Another limitation is related to the correlation equations used in its development. Although the equations were accurate for lower strength steels, except for the elongation equation, they do not fully represent the properties at higher strengths. This is because at lower strengths, the correlation between the alloy's hardness

and tensile strength converged. However, with increasing strength, the correlation diverged, resulting in the lower accuracies. As such, the type of equation used heavily influences the accuracy of the results. Lastly, the range of the dataset constrains the ranges of alloying elements and heat treatment conditions that the algorithm can generate. As most of the input data had lower to medium carbon contents, the probability of generating results with such contents was higher than producing results with higher carbon contents. This highlights the need for a more diverse dataset that can encompass a wider range of alloying elements and heat treatment conditions for better optimization results.

While this algorithm has shown promising results in the optimization of mechanical properties and cost, addressing the limitations can lead to further improvements in accuracy and reliability. As such, future research can focus on the following:

- Increasing the dataset to retrain the hardness and microstructure models and fine-tuning the search space for the algorithm to improve accuracy.
- Exploring the use of different correlation equations for hardness and tensile strength as these diverged at higher strengths.
- Obtaining more accurate correlation equations for tensile strength and elongation as the utilized equations led to lower accuracies for predicted elongation.
- Lastly, experimenting with different combinations of cost optimization and other mechanical property optimization weights and exponents to find the best balance.

Chapter 5 Conclusions

5.1 Key Outcomes

This work presented a μGA for cost and mechanical property optimization. Three representative steels were selected to get appropriate target mechanical properties and cost based on standard practice. From this, the algorithm was able to successfully generate steel compositions that met these specifications while minimizing cost production. Ultimately, the following conclusions can be drawn:

- The neural network based computational framework can be successfully employed to obtain optimal combinations of chemical composition and TMP schedules of steels to obtain steels with desired mechanical properties. Additionally, ANNs can also be used to accurately estimate the composition of the microstructure.
- Unlike the traditional GAs, the μGA proposed in this work is less complex to implement and can obtain feasible solutions over much fewer iterations. In other words, the computational cost, mirrored by the number of function evaluations, is much smaller in the μGA framework proposed here. This makes it an excellent tool for a thorough exploration of such a high dimensional search space.
- The cost function formulation allows for an adjustment of the emphasis of the various target values through pre-constant weights, and exponents. For the problem investigated here, an adjustment of exponents resulted in more function evaluations before equilibrium was reached, and the penalty parameters also varied through the

iterations. In other words, the exponents in the cost function formulation are more sensitive and impactful in emphasizing on a target property.

- The range of the input parameters utilized by the algorithm impacts the predictions, regardless of the mechanical property being emphasized. Additionally, in general, the algorithm significantly reduces heat treatment time, leading to overall cost savings.
- Except for E2, the optimal solutions had similar costs. This was mainly due to the correlation equation used to relate TS to TE. Results can be impacted by changing the cost function formulations.

The success of this work has many implications for practical applications, including the development of cost effective and high performing steels. While there are some limitations in the work, such as the accuracy limitations that occur due to the dataset ranges, and correlation equations not accurately representing the properties at higher strength levels, the algorithm presents a promising solution to the mechanical property and cost optimization problem. Through future research, the listed limitations can be solved for more accurate and reliable results.

Overall, this μGA in conjunction with the principles of neural networks provides a novel approach to steel composition design. It offers a cost effective and efficient solution that has numerous applications in research and industry. As such, it has the potential to provide new means of optimization.

5.2 Implications for Practical Applications

Given that the developed algorithm showed high potential for mechanical property and cost optimization in new steels, there are several implications in the field of material science and engineering both at the research level within laboratories, and application level within industry. The μGA developed in this research provides an approach to the optimization of steel alloy compositions and heat treatment conditions that meet desired mechanical properties while minimizing the overall cost. This provides an efficient means of quickly searching a large range of possible compositions to identify optimal solutions that result in significant time and cost savings for steel manufacturers as experimental trials for the development of new materials are minimized. Furthermore, these newly developed materials ensure that a more comprehensive database can be stored which could enhance the predictive power of machine learning algorithms used in steel design and optimization and ultimately improving their accuracies allowing for accelerated material discovery. Furthermore, the amount of waste generated during material production could potentially decrease as the algorithm is used as a tool to design material with specific material property target rather than through trial and error. This would lead to improved sustainability through the decrease in waste production as well as the reduction of energy consumption as the design of new materials is more streamlined.

Moreover, further avenues for research and development in this area are opened with this implementation. For example, the use of this algorithm can be extended to optimize for other mechanical properties such as toughness, corrosion, ductility etc. with either more data or with the implementation of correlation equations. Or this approach

could also be applied to other material systems such as polymers and ceramics, allowing for its benefits to be passed on to these applications. It could also be adapted to include other alloying elements or heat treatment conditions for more accuracy.

Ultimately, the successful application of the developed μGA allows for the significant reduction of time and cost required for material development and the potential to extend beyond the steel industry into other applications. Further, by combining machine learning with this optimization, the development of new materials is accelerated, therefore improving the manufacturing process while reducing its environmental impact.

5.3 Recommendations for Future Research

While the implementation of the μGA within this research achieved its objectives, there are still areas that require research to improve the results. Below are some recommendations for future research that could enhance the performance of the developed μGA and potentially allow for more applicability in industry.

1. As this methodology relies heavily on the type of data used for training the developed NN models for prediction, future research could explore how an increase in the input dataset would affect the predictions for low, medium, and high strength steels. Moreover, studies could also focus on determining the minimum required data that would produce accurate results in cases when a large dataset is not readily available.
2. The impact on expanding the search space by including additional alloying elements or getting steels with varying compositions of alloys such as phosphorus, sulfur, aluminium, titanium, could be studied.

3. The results from the μGA could be compared to other optimization techniques such as gradient descent methods or hybrid optimization methods discussed within such that their strengths and weakness are outlined and their effectiveness, based on input parameters, examined.
4. Additionally, physical experiments could be conducted to validate the suggest input characteristics retrieved from the μGAs. This could potentially involve fabricating and testing the samples to confirm that they exhibit the predicted mechanical properties and microstructure.
5. Finally, the developed algorithms could also be applied to available current industrial dataset to further confirm its optimization ability.

Appendix A Neural Network

A.1 Hyperparameters

This section outlines the parameters used to train both the ROH and microstructure prediction models. To better handle outliers during the analysis, Huber's loss was selected over the Mean Squared Error (MSE) loss [39]. The results obtained from implementing these parameters are presented in Section A.2. The selected hyperparameters for both models are shown in Table A-1.

Table A-1: Hardness Model Hyperparameters

Parameter	**ROH Model Values**	**Microstructure Prediction Model Values**
Batch Size	256	32
Epoch	5000	100
Learning Rate	0.003	
Optimizer	RMSProp	
Loss	Huber	

A.2 Training and Testing

The development of the hardness and microstructure prediction models involved training using 80% of the randomized and normalized input data. The remaining 20% was used for testing the created models. To verify the consistency of these models, a cross validation approach was performed on the ROH model. This cross validation was carried out for five folds and the results are shown in Table A-2. Overall, this resulted in a mean

R^2 score of 0.97 validating the model and giving confidence to incorporate it into the optimization algorithm.

Table A-2: Cross Validation Results for the ROH model

Cross Validation Folds	**R^2 Score**
1	0.98
2	0.97
3	0.98
4	0.97
5	0.97
Overall	**0.97 Mean (0.00 STD)**

Demonstrating a high level of accuracy in predicting hardness values based on a population input, the resulting R^2 score for the testing set was 0.99. This indicated that the model could consistently and reliably predict hardness values. This accuracy is illustrated in Figure A-1, which presents a comparison between the predicted hardness values versus the actual values.

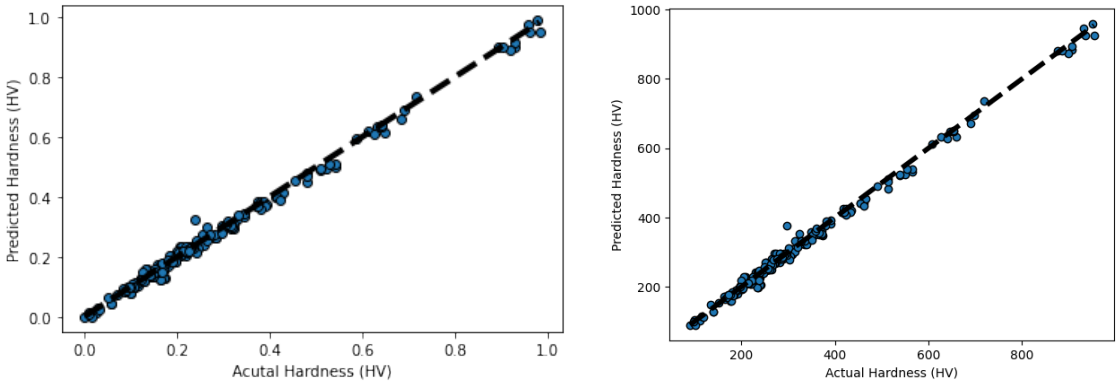

(a) (b)

Figure A-1: Actual and Predicted Hardness Values as Predicted by the ROH Model: (a) Normalized Results and (b) Rescaled Results

For the microstructure prediction model, a MSE rather than an R^2 score was used to show its accuracy since this model predicted more than 1 outcome. These results, shown in Table A-3 and Figure A-2, show that all MSE values were near zero, indicating a high level of accuracy in the model's predictions. However, it should be noted that characterizing the austenite microstructure was challenging due to the limited diversity in the original dataset.

Table A-3: MSE Results from the Microstructure Prediction Model for Austenite, Ferrite, Pearlite, Bainite, and Martensite.

Microstructure	**MSE Value[1]**
Austenite	0.003
Ferrite	0.005
Pearlite	0.005
Bainite	0.008
Martensite	0.007

[1] This value was based on the normalized results. Meaning, the values had not been scaled back to their original values.

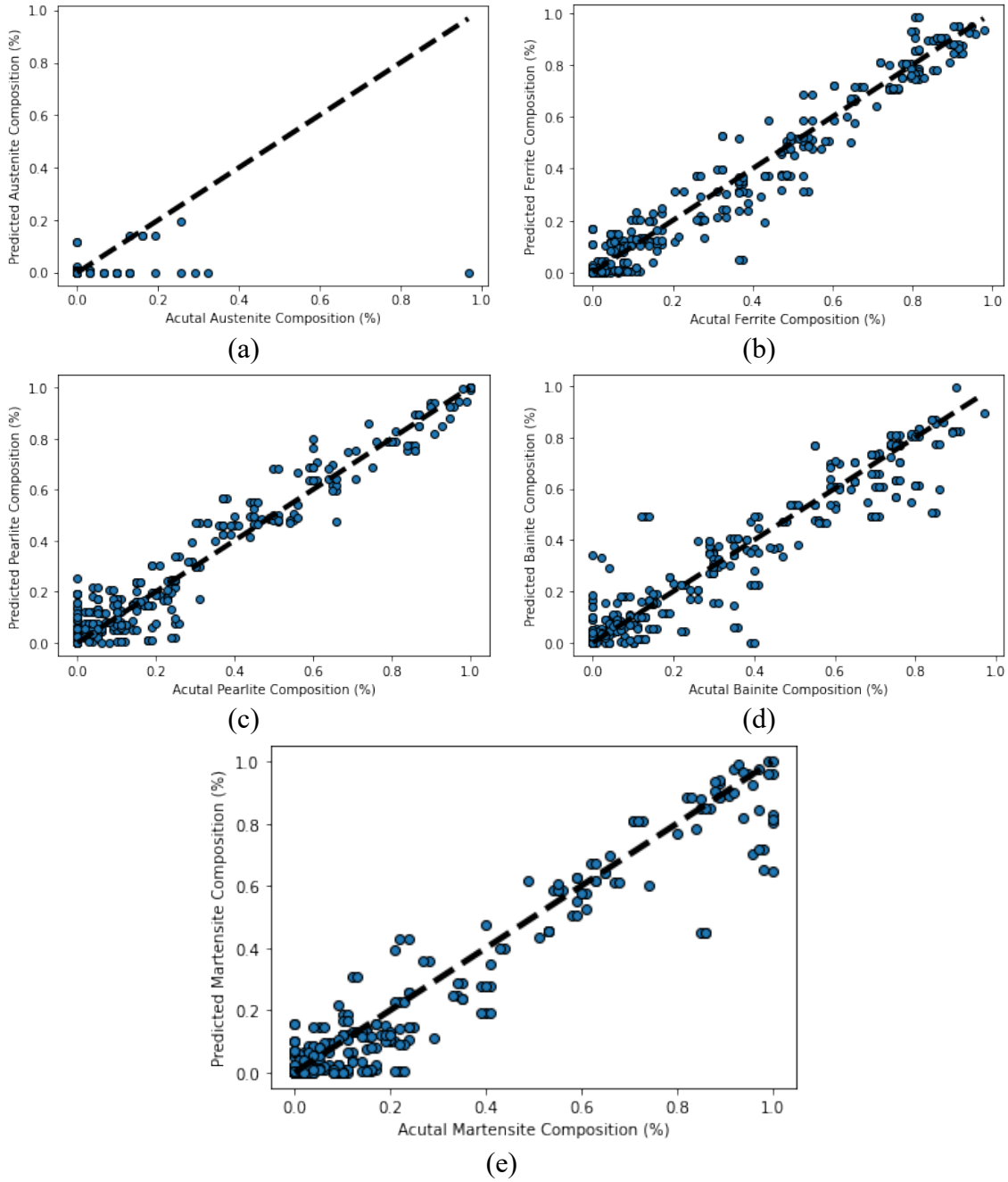

Figure A-2: Actual and Predicted Microstructure Values as Predicted by the Microstructure Prediction Model: (a) Austenite Predicted Results, (b) Ferrite Predicted Results, (c) Pearlite Predicted Results, (d) Bainite Predicted Results, and (e) Martensite Predicted Results

Appendix B Pseudo Code

This section provides an overview of the code used in this research to develop the ROH models, the microstructure prediction model, and the μGA. The code serves as a reference to illustrate the basic steps and functions used in each algorithm to outline the underlying logic and methodology.

B.1 ROH Prediction Model

Import relevant libraries
Import sample data

Randomize the imported data
Normalize the data
Split data with 80% training and 20% testing

Initialize Hyperparameters

DEF hardness model () {
    Initialize Sequential Model
    Add dense layer
    Add dense layer
    Apply a Huber loss
    Add Dense Layer
    Compile Model
}

Fit hardness model using training data
Predict from the microstructure model using testing data

Report the predicted hardness, maximum error, and r2 score
Plot the results

B.2 Microstructure Prediction Model

Import relevant libraries
Import sample data

Randomize the imported data
Normalize the data
Split data with 80% training and 20% testing

Initialize Hyperparameters

DEF microstructure model () {
    Initialize Sequential Model
    Add dense layer
    Add dense layer
    Apply a Huber loss
    Add Dense Layer
    Compile Model
}

Fit microstructure model using training data
Predict from the microstructure model using testing data

Report the predicted microstructures, maximum error, and r2 score
Plot the results

B.3 Genetic Algorithm

Import relevant libraries
Import trained ROMs
Variable initialization

DEF Genetic Algorithm () {
    Iterations = 0
    IF first iteration
        Generate N = 5 pupils
        Append the pupils to an empty list
    ELSE
        Generate N = 4 pupils
        Append to list with best pupil from last iterations

    FOR loop over number of pupils
        Evaluate MC for the pupil

    Obtain the predicted hardness using the ROH model
    Calculate TS from the correlation equation
    Calculate TE from the correlation equation

    IF first iteration
        N = 5
    ELSE
        N = 4

    FOR loop over N number of pupils
        Evaluate the objective function for N pupils
        Append the function to a list
        Evaluate and update the penalty parameter

    Obtain the MIN objective function
    keep the MIN objective function's pupil
    Discard the remainder of the pupil from the list
}

Appendix C General Information

C.1 Cost of Electricity

The cost estimation for electricity consumption was calculated to be approximately 0.14 $/kWh. This was computed based on a usage period between 7 am – 5 pm during the winter months (November 1 – April 30). This calculation is shown below. Pricing information based on time of day were obtained from the Ontario Energy Board (OEB) Time-of-Use (TOU) prices [40]. A breakdown of these prices is shown in Table C-1.

$$Cost_{average} = \frac{\sum hours \times \frac{cost}{kWh}}{Total\ \#\ of\ hours}$$

$$cost_{average} = \frac{\left(4\ h \times \frac{\$0.17}{kWh}\right) + \left(6\ h \times \frac{\$0.113}{kWh}\right)}{10\ h} = \frac{\$0.1358}{kWh} = \$0.14/kWh$$

Table C-1: TOU prices as outlined by the OEB

TOU Prices Period	Description of Time	TOU Prices (¢/kWh)
Off-Peak	Weekdays 7 pm – 7 am All day weekends and holidays	8.2
Mid-Peak	Weekdays 11 am – 5 pm.	11.3
On-Peak	Weekdays 7 – 11 am and 5 – 7 pm.	17.0

C.2 Cost of Alloying Elements

The cost associated with each alloying elements used within this research was retrieved from material-properties.org [41] and is presented below.

Table C-2: Cost of Alloying Elements (Retrieved from [41])

Element (wt. %)	Cost ($/100 g)
C	2.40
Mn	1.70
P	4.00
S	24.00
Si	50.00
Ni	7.70
Cr	10.00
Mo	11.00
Cu	2.70
Al	1.80
V	220.00
B	250.00
N	0.40
Ti	6.10
W	11.00

C.3 Software and Hardware Information

Below is a summary of the key platforms and libraries used for the creation of the ANN and the development of the genetic algorithm along with their versions and the hardware it ran on.

Software:

- Python: 3.8.7
- TensorFlow: 2.9.2
- Keras: 2.9.0

SciKit-Learn: 1.0.2

- Pandas: 1.3.5
- Numpy:1.21.6

Hardware:

- ANN
  - Google Colab GPU: Intel Xeon CPU @2.20 GHz
  - System RAM: 12.7 GB
- Genetic Algorithm
  - CPU: 2.3 GHz Quad-Core Intel Core i7
  - System RAM: 32 GB

References

[1] J T. Black and Ronald A. Kohser, 'DeGarmo's Materials and Processes in Manufacturing, 13th Edition | Wiley', *Wiley.com*. https://www.wiley.com/en-us/DeGarmo%27s+Materials+and+Processes+in+Manufacturing%2C+13th+Edition-p-9781119492825 (accessed Oct. 04, 2022).

[2] F. Busetti, 'Genetic Algorithms Overview', 2001.

[3] H. Adeli and Kamal C. Sarma, 'Cost Optimization of Structures: Fuzzy Logic, Genetic Algorithms, and Parallel Computing | Wiley', *Wiley.com*. https://www.wiley.com/en-us/Cost+Optimization+of+Structures%3A+Fuzzy+Logic%2C+Genetic+Algorithms%2C+and+Parallel+Computing-p-9780470867341 (accessed Feb. 21, 2023).

[4] W. C. Leslie, *The Physical Metallurgy of Steels*. Hempisphere Publishing Corporation, 1981.

[5] H. E. Boyer and J. L. Dossett, *Practical Heat Treating*, 2nd ed. ASM International, 2006. Accessed: Oct. 04, 2022. [Online]. Available: https://www.asminternational.org/practical-heat-treating-second-edition/results/-/journal_content/56/05144G/PUBLICATION/

[6] X. Yuan, L. Chen, Y. Zhao, H. Di, and F. Zhu, 'Influence of annealing temperature on mechanical properties and microstructures of a high manganese austenitic steel', *Journal of Materials Processing Technology*, vol. 217, pp. 278–285, Mar. 2015, doi: 10.1016/j.jmatprotec.2014.11.027.

[7] F. Maratray, *High carbon manganese austenitic steels*. Paris: The Institute, 1995.

[8] U. Gürol and S. Kurnaz, 'Effect of carbon and manganese content on the microstructure and mechanical properties of high manganese austenitic steel', *Journal of Mining and Metallurgy, Section B: Metallurgy*, vol. 56, pp. 9–9, Jan. 2020, doi: 10.2298/JMMB191111009G.

[9] M. K. Banerjee, D. Ghosh, and S. Datta, 'Effect of composition and thermomechanical processing on the ageing characteristic of copper-bearing HSLA steel', *Scandinavian Journal of Metallurgy*, vol. 29, no. 5, pp. 213–223, 2000, doi: 10.1034/j.1600-0692.2000.d01-25.x.

[10] S. Torabi, K. Amini, and M. Naseri Seftejani, 'Investigating the Effect of Manganese Content on the Properties of High Manganese Austenitic Steels', *Int J Advanced Design and Manufacturing Technology*, vol. 10, pp. 75–83, Apr. 2017.

[11] A. V. Kushnarev, A. A. Kirichkov, N. V. Koptseva, D. M. Chukin, and M. P. Baryshnikov, 'Structural and phase transformations in the continuous cooling of steel for one-piece railroad wheels', *Steel Transl.*, vol. 44, no. 4, pp. 306–311, Apr. 2014, doi: 10.3103/S0967091214040123.

[12] H. Wang, L. Cao, Y. Li, M. Schneider, E. Detemple, and G. Eggeler, 'Effect of cooling rate on the microstructure and mechanical properties of a low-carbon low-alloyed steel', *J Mater Sci*, vol. 56, no. 18, pp. 11098–11113, Jun. 2021, doi: 10.1007/s10853-021-05974-3.

[13] S. Ojha, N. S. Mishra, and B. K. Jha, 'Effect of cooling rate on the microstructure and mechanical properties of a C–Mn–Cr–B steel', *Bull Mater Sci*, vol. 38, no. 2, pp. 531–536, Apr. 2015, doi: 10.1007/s12034-015-0862-7.

[14] S. Ganguly, S. Datta, and N. Chakraborti, 'Genetic Algorithms in Optimization of Strength and Ductility of Low-Carbon Steels', *Materials and Manufacturing Processes - MATER MANUF PROCESS*, vol. 22, pp. 650–658, Jun. 2007, doi: 10.1080/10426910701323607.

[15] P. Das and S. Datta, 'Exploring the non-linearity in empirical modelling of a steel system using statistical and neural network models', *International Journal of Production Research*, vol. 45, no. 3, pp. 699–717, Feb. 2007, doi: 10.1080/00207540600792465.

[16] T. K. Patra, V. Meenakshisundaram, J.-H. Hung, and D. S. Simmons, 'Neural-Network-Biased Genetic Algorithms for Materials Design: Evolutionary Algorithms That Learn', *ACS Comb. Sci.*, vol. 19, no. 2, pp. 96–107, Feb. 2017, doi: 10.1021/acscombsci.6b00136.

[17] G. Sidhu, S. D. Bhole, D. L. Chen, and E. Essadiqi, 'Development and experimental validation of a neural network model for prediction and analysis of the strength of bainitic steels', *Materials & Design*, vol. 41, pp. 99–107, Oct. 2012, doi: 10.1016/j.matdes.2012.04.027.

[18] J. H. Holland, *Adaptation in Natural and Artificial Systems: An Introductory Analysis with Applications to Biology, Control, and Artificial Intelligence*. 1992. doi: 10.7551/mitpress/1090.001.0001.

[19] K. De Jong, 'Learning with Genetic Algorithms: An Overview', *Machine Learning*, vol. 3, pp. 121–138, Oct. 1988, doi: 10.1007/BF00113894.

[20] Melanie Mitchell, 'Genetic Algorithm: An Overview', *Complexity*, vol. 1, no. 1, pp. 31–39, Oct. 1995, doi: https://doi.org/10.1002/cplx.6130010108.

[21] N. Chakraborti, 'Genetic Algorithms in Materials Design and Processing', *International Materials Reviews*, vol. 49, pp. 246–260, Jun. 2004, doi: 10.1179/095066004225021909.

[22] M. Mahfouf, M. Jamei, and D. A. Linkens, 'Optimal Design of Alloy Steels Using Multiobjective Genetic Algorithms', *Materials and Manufacturing Processes*, vol. 20, no. 3, pp. 553–567, May 2005, doi: 10.1081/AMP-200053580.

[23] S. Srinivasan, S. Bhole, and G. Sidhu, 'An algorithm for optimal design and thermomechanical processing of high carbon bainitic steels', *International Journal of Aerodynamics*, vol. 6, p. 176, Jan. 2018, doi: 10.1504/IJAD.2018.10015274.

[24] A. L.-S. Chua, N. A. Benedek, L. Chen, M. W. Finnis, and A. P. Sutton, 'A genetic algorithm for predicting the structures of interfaces in multicomponent systems', *Nat Mater*, vol. 9, no. 5, pp. 418–422, May 2010, doi: 10.1038/nmat2712.

[25] L. A. Zadeh, 'Fuzzy sets', *Information and Control*, vol. 8, no. 3, pp. 338–353, Jun. 1965, doi: 10.1016/S0019-9958(65)90241-X.

[26] G. Dulikravich and I. Egorov-Yegorov, 'Design of Alloy's Concentrations for Optimized Strength, Temperature, Time-to-Rupture, Cost and Weight', Jan. 2005, doi: 10.7449/2005/Superalloys_2005_419_428.

[27] F. Tanner and S. Srinivasan, 'Global Optimization of a Two-Pulse Fuel Injection Strategy for a Diesel Engine Using Interpolation and a Gradient-Based Method', *SAE Technical Papers*, Apr. 2007, doi: 10.4271/2007-01-0248.

[28] George F. Vander Voort, *Atlas of Time Temperature Diagrams, Two-Volume Set - ASM International*. ASM International, 1991. Accessed: Sep. 26, 2022. [Online]. Available: https://www.asminternational.org/search/-/journal_content/56/10192/06191G/PUBLICATION

[29] E. J. Pavlina and C. J. Van Tyne, 'Correlation of Yield Strength and Tensile Strength with Hardness for Steels', *J. of Materi Eng and Perform*, vol. 17, no. 6, pp. 888–893, Dec. 2008, doi: 10.1007/s11665-008-9225-5.

[30] D. Bhattacharya, 'Microalloyed Steels for the Automotive Industry', *TMM*, vol. 11, no. 4, pp. 371–383, 2014, doi: 10.4322/tmm.2014.052.

[31] D. Matlock, J. Speer, E. Moor, and P. Gibbs, 'Recent developments in advanced high strength sheet steels for automotive applications: An overview', 2012. Accessed: Jan. 05, 2023. [Online]. Available: https://www.semanticscholar.org/paper/JESTECH-RECENT-DEVELOPMENTS-IN-ADVANCED-HIGH-SHEET-Matlock-Speer/2bfca3c314ae862b5d166e9cf36ed1e184dfdb21

[32] A. Barbacki and E. Mikołajski, 'Optimization of heat treatment conditions for maximum toughness of high strength silicon steel', *Journal of Materials Processing Technology*, vol. 78, no. 1, pp. 18–23, Jun. 1998, doi: 10.1016/S0924-0136(97)90457-X.

[33] 'McCormick Function'. https://www.sfu.ca/~ssurjano/mccorm.html (accessed Mar. 04, 2023).

[34] 'Easom Function'. https://www.sfu.ca/~ssurjano/easom.html (accessed Mar. 04, 2023).

[35] 'Ackley Function'. https://www.sfu.ca/~ssurjano/ackley.html (accessed Mar. 27, 2023).

[36] L. Zhang, D. Wu, and Z. Li, 'Influence of Alloying Elements on Mechanical Properties and Corrosion Resistance of Cold Rolled C-Mn-Si TRIP Steels', *Journal of Iron and Steel Research, International*, vol. 19, no. 12, pp. 42–47, Dec. 2012, doi: 10.1016/S1006-706X(13)60030-8.

[37] 'Classification and Designation of Carbon and Low-Alloy Steels', Jan. 1990, doi: 10.31399/asm.hb.v01.a0001009.

[38] W. F. Cannon, 'Manganese: it turns iron into steel (and does so much more)', U.S. Geological Survey, Reston, VA, USGS Numbered Series 2014–3087, 2014. doi: 10.3133/fs20143087.

[39] N. Kapoor, 'Loss Functions -when to use which one', *Numpy Ninja*, Nov. 17, 2020. https://www.numpyninja.com/post/loss-functions-when-to-use-which-one (accessed Apr. 13, 2023).

[40] 'Electricity rates | Ontario Energy Board'. https://www.oeb.ca/consumer-information-and-protection/electricity-rates#current (accessed Oct. 25, 2022).

[41] 'Prices of Chemical Elements - $/kg', *Material Properties*. https://material-properties.org/prices-of-chemical-elements-kg/ (accessed Oct. 25, 2022).